CellPress

Molecular Cell
Letters

Who Is Leading the Replication Fork, Pol ε or Pol δ?

Peter M.J. Burgers,[1] Dmitry Gordenin,[2] and Thomas A. Kunkel[2,*]
[1]Department of Biochemistry and Molecular Biophysics, Washington University School of Medicine, St. Louis, MO 63110, USA
[2]Genome Integrity and Structural Biology Laboratory, National Institute of Environmental Health Sciences, NIH, DHHS, Research Triangle Park, NC 27709, USA
*Correspondence: kunkel@niehs.nih.gov
http://dx.doi.org/10.1016/j.molcel.2016.01.017

Several studies in the past decade support a model wherein DNA polymerase ε (Pol ε) carries out the majority of leading-strand DNA replication of the undamaged eukaryotic nuclear genome. Now a recent paper in *Molecular Cell* from the Prakash laboratory challenges this model, claiming instead that Pol δ is the major replicase for both strands and that Pol ε's primary role is only to proofread errors made by Pol δ during leading-strand replication (Johnson et al., 2015). While we fully subscribe to the idea that the replication fork is plastic and that its composition can adapt to various challenges, we believe the foundation for an unchallenged replication fork remains as established before the Prakash paper, for the following reasons.

Mutation Rate Data

Our studies with mutants of the *POL3* and *POL2* genes encoding the catalytic subunits of Pol δ and Pol ε, respectively, revealed that they have two unique properties that lend themselves to studying strand-specific incorporation during replication. The first is that they are asymmetric mutators. As but one example, for the two mispairs that lead to AT→GC transitions, budding yeast Pol δ containing a L612M mutation in the polymerase active site misincorporates dGMP opposite template T much more frequently than dCMP opposite template A. When we eliminated error correction by deleting the mismatch repair gene *MSH2* (Lujan et al., 2014; Nick McElhinny et al., 2008), the *msh2Δ pol3-L612M* strain exhibited a large synergistic increase in AT→GC transitions compared to the wild-type and *msh2Δ* strains, and relative to known replication origins, these mutations occurred in a pattern consistent with a model wherein Pol δ's primary role is in lagging-strand replication. Importantly, the synergistic increase was very strong, providing confidence that the large majority of the mutations in the *msh2Δ pol3-L612M* strain were indeed due to the Pol δ-L612M change. However, strong mutators rapidly accumulate suppressor mutations that result in wide variations in mutation rates in the mitotic progeny of double mutants. This was obvious in our study of the *msh2Δ pol3-L612M* mutant (see Figure S1 in Nick McElhinny et al., 2008), leading us to quantify mutation rates in cultures obtained by limited outgrowth of haploid spores germinated from meiotic progeny of the heterozygous diploids *pol3-L612M/pol3-L612M MSH2/msh2Δ*. This was not done in the Prakash study. Instead, they obtained double-mutant strains by two subsequent transformations involving several rounds of outgrowth from single cells, and obtained mutation rates that were only a few percent of the high rates we determined. Thus, whether from accumulating suppressor mutations during extensive propagation or for other reasons, their strains lack the high mutation rates we used to assign mutations specifically to Pol δ-L612M errors. In addition, their mutational spectrum for one orientation of *URA3* in the S288c background shows strong GC→TA hotspots at base pairs 679 and 706 in *URA3* that together constitute a third of the observed mutations. The authors suggest that those substitutions preferentially originated from template G-dAMP mismatches. However, those two hotspots are missing in a strain having *URA3* in the opposite orientation. This would lead to the paradoxical suggestion that Pol δ-L612M does not replicate the lagging strain, yet neither they nor we imply that this is the case. Instead, our data suggest that the majority of GC→TA mutations in undamaged cells actually result from the complementary C-dTMP mismatch (Lujan et al., 2014; Nick McElhinny et al., 2008). Therefore, we conclude that those two mutation hotspots, and by extension other hotspots, support, rather than disprove, our favored model.

Asymmetric Ribonucleotide Incorporation

A second useful feature of Pol δ and Pol ε variants is that they increase the incorporation of ribonucleotides into DNA. This occurs in vitro and in yeast in which newly incorporated ribonucleotides remain in the genomes of RNase H2-deficient (*rnh201Δ*) strains that are defective for ribonucleotide excision repair. Mapping data using next-generation sequencing shows increased ribonucleotide incorporation into the nascent lagging strand for *pol3-L612M/G* budding yeast variants and for an equivalent fission yeast variant, and increased ribonucleotide incorporation into the nascent leading strand of the *pol2-M644G* variant and its fission yeast equivalent (Clausen et al., 2015; Daigaku et al., 2015; Koh et al., 2015; Reijns et al., 2015). The straightforward explanation of these results is that Pol ε primarily replicates the leading strand and Pol δ primarily replicates the lagging strand. The Prakash study offers the alternative explanation that Pol ε does not incorporate ribonucleotides during replication, but rather only proofreads ribonucleotides incorporated by *pol3-L612M*, and does so only during leading-strand replication. However, Pol δ itself has little or no ability to proofread DNA termini containing ribonucleotides, but it can extend them, so there is no reason for Pol δ to dissociate to allow Pol ε to gain access to these termini. Moreover, while Pol ε can intrinsically proofread its own mistakes, current evidence suggests that it has little or no ability to extrinsically

proofread mistakes made by Pol δ (Flood et al., 2015). Finally, if Pol ε was important only for proofreading ribonucleotides incorporated by Pol δ into the nascent leading strand, then in an *rnh201Δ* strain with wild-type polymerases, the ribonucleotide density in the nascent leading strand should be lower than in the nascent lagging strand, whereas it is actually higher (Clausen et al., 2015). These facts do not fit a model in which Pol δ is normally the primary leading-strand replicase. However, they do fit a model wherein Pol ε is the major leading-strand replicase, and this role is supported by elegant DNA replication studies in vitro (e.g., see Georgescu et al., 2014). As discussed (Kunkel and Burgers, 2008), our favored model wherein Pol ε is the primary leading-strand replicase does not exclude an important role for Pol δ in leading-strand replication in certain regions of the undamaged genome and/or when the genome is under stress.

REFERENCES

Clausen, A.R., Lujan, S.A., Burkholder, A.B., Orebaugh, C.D., Williams, J.S., Clausen, M.F., Malc, E.P., Mieczkowski, P.A., Fargo, D.C., Smith, D.J., and Kunkel, T.A. (2015). Nat. Struct. Mol. Biol. *22*, 185–191.

Daigaku, Y., Keszthelyi, A., Müller, C.A., Miyabe, I., Brooks, T., Retkute, R., Hubank, M., Nieduszynski, C.A., and Carr, A.M. (2015). Nat. Struct. Mol. Biol. *22*, 192–198.

Flood, C.L., Rodriguez, G.P., Bao, G., Shockley, A.H., Kow, Y.W., and Crouse, G.F. (2015). PLoS Genet. *11*, e1005049.

Georgescu, R.E., Langston, L., Yao, N.Y., Yurieva, O., Zhang, D., Finkelstein, J., Agarwal, T., and O'Donnell, M.E. (2014). Nat. Struct. Mol. Biol. *21*, 664–670.

Johnson, R.E., Klassen, R., Prakash, L., and Prakash, S. (2015). Mol. Cell *59*, 163–175.

Koh, K.D., Balachander, S., Hesselberth, J.R., and Storici, F. (2015). Nat. Methods *12*, 251–257, 253 p following 257.

Kunkel, T.A., and Burgers, P.M. (2008). Trends Cell Biol. *18*, 521–527.

Lujan, S.A., Clausen, A.R., Clark, A.B., MacAlpine, H.K., MacAlpine, D.M., Malc, E.P., Mieczkowski, P.A., Burkholder, A.B., Fargo, D.C., Gordenin, D.A., and Kunkel, T.A. (2014). Genome Res. *24*, 1751–1764.

Nick McElhinny, S.A., Gordenin, D.A., Stith, C.M., Burgers, P.M., and Kunkel, T.A. (2008). Mol. Cell *30*, 137–144.

Reijns, M.A., Kemp, H., Ding, J., de Procé, S.M., Jackson, A.P., and Taylor, M.S. (2015). Nature *518*, 502–506.

CellPress

Molecular Cell
Letters

Response to Burgers et al.

Robert E. Johnson,[1,2] Roland Klassen,[1,2,3] Louise Prakash,[1] and Satya Prakash[1,*]
[1]Department of Biochemistry and Molecular Biology, University of Texas Medical Branch, Galveston, TX 77555-1061, USA
[2]Co-first author
[3]Present address: Institut für Biologie, FG Mikrobiologie, Universität Kassel, Kassel D-34132, Germany
*Correspondence: s.prakash@utmb.edu
http://dx.doi.org/10.1016/j.molcel.2016.01.018

In our study (Johnson et al., 2015), we concluded that DNA polymerase (Pol) δ replicates both the leading and lagging DNA strands and that Polε plays no significant role in leading-strand replication. In their Letter in this issue of *Molecular Cell*, Burgers et al. (2016) contend that their model wherein Polε primarily replicates the leading strand still remains valid and suggest that (1) our strains contain suppressors, (2) our observed G→T mutations originate in the lagging strand, and (3) ribonucleotide incorporation data support their model.

Analysis of Mutation Rates and Mutation Spectra

The Kunkel group analyzed mutation rates in haploid spores derived from their yeast strain ΔI(−2)I-7B-YUNI300 because their *pol3-L612M msh2Δ* strain exhibits growth defects and heterogeneous colony size and because such growth defects can give rise to suppressor mutations. However, our *pol3-L612M msh2Δ* strains displayed no growth defects in either the S288C or the DBY747 background, nor in the *pol3-L612M msh2Δ* double mutants obtained by tetrad analysis of *POL3/pol3-L612M MSH2/msh2Δ* diploids (Figure S5 in Johnson et al., 2015). We show that in the *pol3-L612M S288C* strain, Polδ signature errors are detectable only in the lagging strand, whereas in the *pol3-L612M msh2Δ* strain, they also accumulate on the leading strand. Since in the *pol3-L612M msh2Δ* strain ~80% of all mutations are L612M-Polδ signature mutations, a large majority of mutations in this strain represent Polδ-generated errors during replication. Moreover, since suppression could explain the reduced but not the highly increased leading-strand signature mutations of L612M-Polδ that we observe in the *pol3-L612M msh2Δ* strain (see below), suppression is not affecting any of our conclusions for Polδ's role in replication.

Kunkel and colleagues state that since the G→T hotspots at base pairs 679 and 706 are missing in our strain having *URA3* in the opposite orientation, this would lead to the paradoxical suggestion that L612M-Polδ does not replicate the lagging strand. However, such orientation dependence of hotspot errors can be seen in the study by Kunkel and colleagues; although there is a strong T→C hotspot at position 97 in OR1 in *URA3*, this hotspot is missing in *URA3* in the opposite orientation, and no complementary A→G mutations were observed (Nick McElhinny et al., 2008). In our paper, we stress the point that although the L612M-Polδ-generated hotspot mutations occur on both the DNA strands in the *pol3-L612M msh2Δ* S288C strain, the sites at which hotspot mutations occur differ in an orientation-dependent manner, and mismatch repair (MMR) and L612M-Polδ mispair generation can act differentially at different sites during replication of the two DNA strands. Furthermore, differential contribution of MMR and other mismatch removal processes can account for the variability in the level of increase in mutation rates in different yeast strains (Johnson et al., 2015).

Even though we observe a large increase in the rate of G→T hotspot mutations at base pairs 679 and 706 in *URA3*, which we attribute to errors made by Polδ during leading strand replication (see Figure 2B in Johnson et al., 2015), Kunkel and colleagues contend that these mutations arise from C:dTTP mispair formation on the lagging strand; but they provide no rationale for this. In their biochemical studies, they showed that L612M-Polδ exhibits an 8.5:1 bias for G:dATP mispair formation over the C:dTTP mispair (Nick McElhinny et al., 2007), and we independently confirmed this in the sequence context of position 679 in *URA3* (see Figures S2C and S2D in Johnson et al., 2015). Therefore, their claim that the observed G→T mutations derive from C:dTTP mispairs on the lagging strand is not supported by experimental evidence. In their recent study which analyzed the whole-genome sequence of a *pol3-L612M msh2Δ* homozygous diploid, they identified strand-specific G→T mutations near origins. The G:dATP bias predicts that these mutations arise primarily from G:dATP mispair formation on the leading strand, and not from C:dTTP mispair formation on the lagging strand, as they suggest (Lujan et al., 2014). Thus, even in their strain, there is evidence for leading-strand replication by Polδ.

We provide extensive evidence for the various L612M-Polδ signature mutations on both DNA strands in the *pol3-L612M msh2Δ* S288C strain and also in the *pol3-L612M msh2Δ* DBY747 strain in which *URA3* was integrated at many different genomic locations. Altogether, our data support the conclusion that Polδ replicates both the DNA strands. Furthermore, since Polε signature errors on the leading strand do not occur in the *pol2-M644G msh2Δ* strain, Polε plays little if any role in leading-strand replication (Johnson et al., 2015).

Interpretation of Asymmetric Ribonucleotide Incorporation

In view of our data (Johnson et al., 2015), we consider it highly likely that explanations other than a role of Polε in the replication of the leading strand account for the increase in ribonucleotides on the nascent leading strand in the RNase H2-deficient *pol2-M644G* mutant. We suggested in our paper that in yeast strains harboring the *pol2-M644G* mutation, because of the greatly enhanced capacity of the M644G-Polε over wild-type Polδ (~50-fold) to incorporate

ribonucleotides and to extend synthesis from them (Lujan et al., 2013), the mutant Polε takes over synthesis from Polδ and promotes the persistence of ribonucleotides incorporated by Polδ on the leading strand. Moreover, since checkpoint pathways are activated and dNTP levels are elevated in *pol2-M644G* cells (Williams et al., 2015), these factors would contribute to a further increase in the proficiency of mutant Polε to extend synthesis from ribonucleotides.

As for the observation that in the *pol3-L612M rnh201Δ* strain enhanced ribonucleotide incorporation is detected on the lagging strand, we suggest that even though Polδ incorporates ribonucleotides on both the DNA strands, they are more efficiently removed from the leading strand by competing pathways. The identity of these pathways remains to be determined, but because Polε exonuclease can excise ribonucleotides (Williams et al., 2012), this proofreading exonuclease may also act in one such competing pathway. Contrary to their statement that Polε does not proofread mistakes made by Polδ, we provide evidence for Polε exonuclease in removing Polδ errors (see Table 1 in Johnson et al., 2015). Burgers et al. (2016) support their statement by citing a recent study Flood et al. (2015), which is based on an a priori assumption that Polδ replicates the lagging strand and that Polε replicates the leading strand, and it was not designed to directly test the role of Polε exonuclease in removing Polδ-generated mispairs from the leading strand, as we have done.

Without a more complete understanding of the roles of Polδ and Polε in ribonucleotide incorporation and the roles of ribonucleotide removal pathways on each DNA strand, it seems inappropriate to dismiss the evidence indicating a role of Polδ, but not of Polε, in replicating the leading strand, and to selectively use the ribonucleotide incorporation data to propose a role for Polε in replicating the leading strand.

While in vitro studies support an ability of Polε to carry out DNA synthesis on the leading strand (Georgescu et al., 2014), it remains possible that such studies fail to recapitulate all the molecular complexities that occur during replication. Polε plays an essential role in the assembly and progression of CMG helicase on the leading strand, but its polymerase function is dispensable for viability. We have suggested a role for its polymerase activity in rescuing the replication fork at sites where Polδ stalls on the leading strand and in other DNA repair processes, and for its proofreading activity in the removal of Polδ-generated errors (Johnson et al., 2015). The elucidation of these and other Polε roles would require a thorough genetic and molecular analysis of the complexities that underlie these Polε functions.

AUTHOR CONTRIBUTIONS

R.E.J. and R.K. analyzed data. R.E.J., R.K., L.P., and S.P. interpreted results and wrote the letter.

REFERENCES

Burgers, P.M.J., Gordenin, D.A., and Kunkel, T.A. (2016). Mol. Cell *61*, this issue, 492–493.

Flood, C.L., Rodriguez, G.P., Bao, G., Shockley, A.H., Kow, Y.W., and Crouse, G.F. (2015). PLoS Genet. *11*, e1005049.

Georgescu, R.E., Langston, L., Yao, N.Y., Yurieva, O., Zhang, D., Finkelstein, J., Agarwal, T., and O'Donnell, M.E. (2014). Nat. Struct. Mol. Biol. *21*, 664–670.

Johnson, R.E., Klassen, R., Prakash, L., and Prakash, S. (2015). Mol. Cell *59*, 163–175.

Lujan, S.A., Williams, J.S., Clausen, A.R., Clark, A.B., and Kunkel, T.A. (2013). Mol. Cell *50*, 437–443.

Lujan, S.A., Clausen, A.R., Clark, A.B., MacAlpine, H.K., MacAlpine, D.M., Malc, E.P., Mieczkowski, P.A., Burkholder, A.B., Fargo, D.C., Gordenin, D.A., and Kunkel, T.A. (2014). Genome Res. *24*, 1751–1764.

Nick McElhinny, S.A., Stith, C.M., Burgers, P.M., and Kunkel, T.A. (2007). J. Biol. Chem. *282*, 2324–2332.

Nick McElhinny, S.A., Gordenin, D.A., Stith, C.M., Burgers, P.M.J., and Kunkel, T.A. (2008). Mol. Cell *30*, 137–144.

Williams, J.S., Clausen, A.R., Nick McElhinny, S.A., Watts, B.E., Johansson, E., and Kunkel, T.A. (2012). DNA Repair (Amst.) *11*, 649–656.

Williams, L.N., Marjavaara, L., Knowels, G.M., Schultz, E.M., Fox, E.J., Chabes, A., and Herr, A.J. (2015). Proc. Natl. Acad. Sci. USA *112*, E2457–E2466.

CellPress

Reconsidering DNA Polymerases at the Replication Fork in Eukaryotes

Bruce Stillman[1,*]
[1]Cold Spring Harbor Laboratory, 1 Bungtown Road, Cold Spring Harbor, NY 11724, USA
*Correspondence: stillman@cshl.edu
http://dx.doi.org/10.1016/j.molcel.2015.07.004

The distribution of DNA polymerase activities at the eukaryotic DNA replication fork was "established," but recent genetic studies in this issue of *Molecular Cell* raise questions about which polymerases are copying the leading and lagging strand templates (Johnson et al, 2015).

"Everything is complicated. If it were not so, life and poetry and everything else would be a bore." Based on recent literature (Johnson et al, 2015), one could conclude that the molecular events at eukaryotic DNA replication forks, particularly how various DNA polymerases combine to copy both the leading and lagging stand templates, are far from boring, but indeed downright complicated.

Because the two strands of the DNA double helix have opposite polarity and all DNA polymerases replicate in the same direction (5′ to 3′), DNA replication occurs continuously on one strand, the leading strand, but discontinuously via short Okazaki fragments on the other strand, the lagging strand. The different strategies have consequences for the machineries that copy the strands, including which DNA polymerases are involved and also how DNA damage can be repaired.

This entire issue came to the fore when, in addition to DNA polymerases α and δ, a third "replicative" DNA polymerase, polymerase ε, was identified in the yeast *S. cerevisiae* and later found to be conserved in all eukaryotes (Johansson and Dixon, 2013). DNA polymerases α and δ are sufficient to replicate the Simian Virus 40 genome (Figure 1A), long thought of as a model for the eukaryotic DNA replication fork (Waga and Stillman, 1998). A role for DNA polymerase ε proved to be perplexing because the *POL2* gene encoding the largest subunit of the four-subunit DNA polymerase ε is essential, but its N-terminal DNA polymerase catalytic activity can be deleted and yeast are still viable. The essential activity actually lies within the Pol2 C-terminal domain that is involved in the intra-S phase detection of DNA damage and induction of checkpoint signaling to repair damage and maintain fork stability (Dua et al., 1999).

The assignment of DNA polymerases to specific strands during DNA replication in eukaryotic cells has been studied by using mutant versions of DNA polymerases δ and ε with specific error signatures (reviewed in Johansson and Dixon, 2013; Williams and Kunkel, 2014). The studies showed, apparently clearly, that polymerase ε replicated the leading strand and polymerase δ replicated the lagging strand (Figure 1B).

Recent biochemical studies have shown that DNA polymerases α and ε, but not δ, are necessary and sufficient for the initiation of DNA replication at origins of DNA replication (Yeeles et al., 2015), but these in vitro observations do not address the strand assignment for complete DNA replication in vivo. Other biochemical studies from the O'Donnell laboratory have reconstituted DNA replication of leading and lagging strands, assigning DNA polymerase ε for leading-strand synthesis and polymerase δ for lagging-strand synthesis (Georgescu et al., 2014, 2015). They even identified a mechanism that prevents polymerase δ from competing with polymerase ε on the leading strand. Moreover, the structure of polymerase ε shows that it can tightly clamp onto DNA even without PCNA, making it an excellent candidate for the leading-strand polymerase (Hogg et al., 2014). But PCNA may still be required on the leading stand to enable coupling of nucleosome assembly by CAF-1 and other PCNA-associated functions (Figure 1B). Moreover, polymerase ε is directly associated with the CMG (Cdc45-Mcm2-7-GINS) helicase that travels on the leading-strand template DNA (Johansson and Dixon, 2013). Thus, the distribution of labor for polymerases δ and ε makes biochemical sense. Indeed, polymerase ε is enriched on the leading strand and polymerase δ on the lagging strand in vivo (Yu et al., 2014), but an excess of DNA polymerase δ on the lagging would be expected even if polymerase δ replicated both strands since more polymerase molecules are required on the discontinuously synthesized lagging strand. Nevertheless, from genetic and biochemical analysis, it seemed very clear that polymerase ε primarily replicates the leading strand and polymerase δ the lagging strand.

However, the paper by Johnson et al. (2015) in this issue raises the entire question of strand assignments again and concludes that polymerase δ replicates both leading and lagging strands, just like the SV40 model (Figure 1C, normal mode). They attribute the different genetic results to the use of different strains of yeast and to different pathways for repair of misincorporated nucleotides on the leading versus the lagging strand.

Error correction on the leading and lagging strands is likely to be different since the mechanisms of DNA synthesis are different. Johnson et al. suggest that mismatch repair is different on the lagging strand compared to the leading strand—notably that the proofreading activity of DNA polymerase ε is redundant with the exonuclease Exo1 for error repair on the leading stand, but not on the lagging strand. They suggest that the different mismatch repair mechanisms on the leading and lagging strands, coupled with the strains employed can explain the different results.

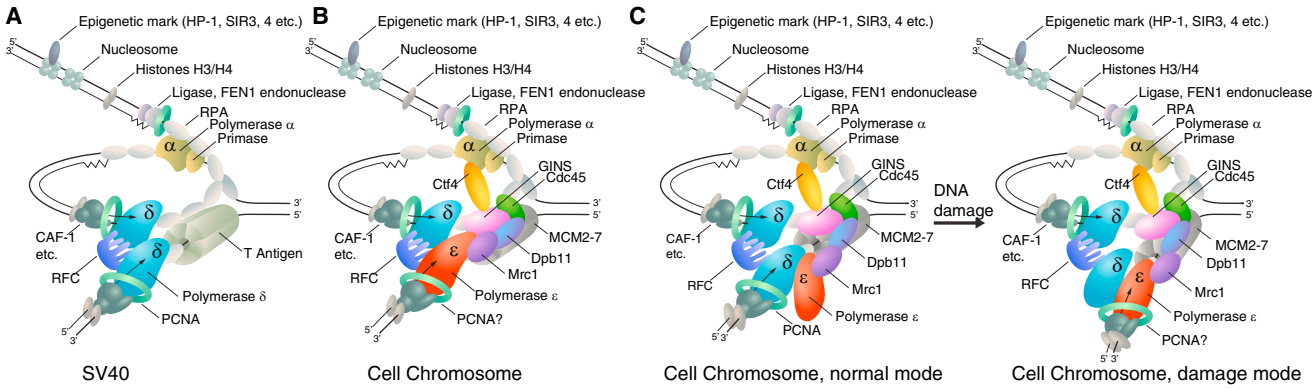

Figure 1. DNA Polymerases at the Eukaryotic DNA Replication Fork

(A) DNA polymerase δ synthesizes DNA during lagging (discontinuously synthesized, top) and leading (continuously synthesized, bottom) replication.

(B) The prevailing model in which DNA polymerase δ synthesizes the lagging strand and polymerase ε the leading strand.

(C) A potential new model in which DNA polymerase δ normally replicates both strands and, upon DNA damage in the leading strand template, a switch to polymerase ε occurs, linking DNA-damage detection to the essential role for polymerase ε and associated checkpoint proteins. In all cases, DNA polymerase α is coupled with primase to synthesize a RNA-DNA primer on the lagging strand that is recognized by RFC and PCNA to switch to the replicative polymerase. PCNA couples other events at the replication fork, such as nucleosome assembly.

Evidence that polymerase ε primarily replicates the leading strand also emerged from data showing that ribonucleotides (rNMPs) were preferentially incorporated into the leading strand during DNA replication, in both *S. cerevisiae* and *S. pombe* (reviewed in Jinks-Robertson and Klein, 2015). These data include very impressive whole-genome analyses of rNMP incorporation into the leading strand when a mutant polymerase ε that promiscuously inserted rNMPs into DNA was employed. Importantly, a strain containing an allele of polymerase ε that was more stringent in rNMP discrimination than the wild-type polymerase ε incorporated less rNMP into the leading strand than the strain with the error-prone polymerase ε. In contrast, when error-prone polymerases α and polymerase δ were present, rNMP incorporation was detected in the lagging strand. So this data seems to strongly support the model shown in Figure 1B. But a third model has now been suggested, namely that polymerase δ normally replicates both strands of the DNA, but that occasionally a switch to polymerase ε on the leading strand can be induced by replication errors, thereby coupling checkpoint signaling to repair of the DNA damage (Figure 1C). This model may explain why mutations in the polymerase ε catalytic residues have a dominant negative effect, suggesting that this inactive polymerase gums up replication (Dua et al., 1999).

The experiments showing preferential incorporation of rNMPs experiments were done in strains lacking the RNase2 enzyme that normally nicks the DNA 5′ to the rNMP in the DNA, creating a 3′-OH that is preferentially extended by DNA polymerase δ, creating a flap for rNMP excision much like strand displacement mechanisms used on the lagging strand. The absence of RNase2 causes extensive replicative stress (reviewed by Williams and Kunkel, 2014), activating the DNA-damage response pathway involving the essential domain of the polymerase ε large subunit. It is therefore possible that in the absence of RNase2, when polymerase δ incorporates an rNMP during leading-strand replication, it stimulates an alternative rNMP repair pathway that involves switching to polymerase ε to remove the rNMP or repair topoisomerase 1 induced DNA damage (Figure 1C). Such a repair mechanism by polymerase ε would only work on the leading strand where it is physically located; thus, rNMPs would be incorporated into that strand during the repair process when an error prone polymerase ε is present. When an error-prone DNA polymerase δ strain is employed, such errors would be repaired by the wild-type polymerase ε, leaving little trace of rNMP on the leading strand. Consistent with this model, on the lagging strand, preferential rNMP incorporation would be detected only in strains with either an error-prone polymerase δ since polymerase ε does not operate on the lagging strand for DNA synthesis or repair. Thus, the data could be construed as supporting the model in Figure 1C where polymerase δ replicates both strands but polymerase ε preferentially ensures leading-strand fidelity.

If the model in Figure 1C is correct, then genetic stability on the leading strand and lagging strand would be different due to the different repair pathways employed. For example, the location of polymerase ε-associated checkpoint proteins such as Mrc1, Dpb11, and Drc1/Sld2 (Osborn et al., 2002) could preferentially signal DNA damage that occurs on the leading strand. DNA-damage-dependent polymerase switching could also promote programed switches in gene expression such as mating type gene in *S. pombe* (see Williams and Kunkel, 2014). Such imprinting is thought to be marked by an rNMP-containing gap in the leading-strand template DNA, and recognition of this gap by the replicative helicase or polymerase may trigger a switch to DNA polymerase ε-coupled recombination.

The new paper by Johnson et al. will generate much discussion, and the polymerase assignment debate will continue. But, importantly, all of the genetic studies dealing with this issue, including those of Johnson et al., employ mutant strains that inform what is going on in the mutant condition (including all genetic variation in

CellPress

the strains used), suggesting caution about interpreting what is really going on in wild-type cells.

ACKNOWLEDGMENTS

Research in the author's laboratory is supported by NIH grants (GM45436 and CA13106). I thank Julia Kuhl for artwork.

REFERENCES

Dua, R., Levy, D.L., and Campbell, J.L. (1999). J. Biol. Chem. *274*, 22283–22288.

Georgescu, R.E., Langston, L., Yao, N.Y., Yurieva, O., Zhang, D., Finkelstein, J., Agarwal, T., and O'Donnell, M.E. (2014). Nat. Struct. Mol. Biol. *21*, 664–670.

Georgescu, R.E., Schauer, G.D., Yao, N.Y., Langston, L.D., Yurieva, O., Zhang, D., Finkelstein, J., and O'Donnell, M.E. (2015). Elife *4*, e04988.

Hogg, M., Osterman, P., Bylund, G.O., Ganai, R.A., Lundström, E.B., Sauer-Eriksson, A.E., and Johansson, E. (2014). Nat. Struct. Mol. Biol. *21*, 49–55.

Jinks-Robertson, S., and Klein, H.L. (2015). Nat. Struct. Mol. Biol. *22*, 176–178.

Johansson, E., and Dixon, N. (2013). Cold Spring Harb. Perspect. Biol. *5*, a012799.

Johnson, R.E., Klassen, R., Prakash, L., and Prakash, S. (2015). Mol. Cell *59*, this issue, 163–175.

Osborn, A.J., Elledge, S.J., and Zou, L. (2002). Trends Cell Biol. *12*, 509–516.

Waga, S., and Stillman, B. (1998). Annu. Rev. Biochem. *67*, 721–751.

Williams, J.S., and Kunkel, T.A. (2014). DNA Repair (Amst.) *19*, 27–37.

Yeeles, J.T., Deegan, T.D., Janska, A., Early, A., and Diffley, J.F. (2015). Nature *519*, 431–435.

Yu, C., Gan, H., Han, J., Zhou, Z.X., Jia, S., Chabes, A., Farrugia, G., Ordog, T., and Zhang, Z. (2014). Mol. Cell *56*, 551–563.

Tailoring MicroRNA Function: The Role of Uridylation in Antagonizing Mirtron Expression

Olivia S. Rissland[1,2,*]
[1]Molecular Structure and Function Program, The Hospital for Sick Children Research Institute, Toronto, ON, Canada M5G 0A4
[2]Department of Molecular Genetics, University of Toronto, Toronto, ON, Canada M5S 1A8
*Correspondence: olivia.rissland@sickkids.ca
http://dx.doi.org/10.1016/j.molcel.2015.07.001

In this issue of *Molecular Cell*, Bortolamiol-Becet et al. (2015) and Reimão-Pinto et al. (2015) show that in flies Tailor preferentially uridylates mirtron pre-miRNA hairpins to suppress their biogenesis.

3′ end modifications are a recurring theme in RNA regulation. Often acting as an RNA analog of ubiquitin, they regulate small RNA abundance at several points in the microRNA (miRNA) life cycle (Scott and Norbury, 2013). Animal miRNAs are first processed in the nucleus by Drosha (Figure 1). The liberated pre-miRNA hairpin is then cleaved in the cytoplasm by Dicer. One strand of the resultant duplex, the mature miRNA, is loaded into Argonaute, where it directs repression of target mRNAs.

Uridylation and adenylation regulate both pre-miRNAs and miRNAs. In mammals, the terminal(U) transferase TUT4, recruited by Lin28, oligouridylates pre-let-7 to inhibit dicing and provide a landing platform for the exonuclease Dis3l2 (Chang et al., 2013; Kim et al., 2010). In the absence of Lin28, mono- and di-uridylation of pre-miRNAs can enhance dicing of some let-7 family members (Scott and Norbury, 2013). Mature miRNAs are also subject to 3′ end modifications, which typically stimulate their decay. For instance, in flies and humans, miRNAs, when bound to highly complementary targets, are degraded through the trimming and tailing pathway (Ameres et al., 2010). Other, target-independent, decay pathways exist, but these are less well understood (Kim et al., 2010; Lee et al., 2014).

There are additional, productive variations of the miRNA biogenesis pathway (Yang and Lai, 2011). One such pathway bypasses Drosha cleavage and instead uses splicing and subsequent lariat debranching to generate the pre-miRNA hairpin (Figure 1). These miRNAs are called "mirtrons" and have been found in flies, worms, and humans (Yang and Lai, 2011). Because intron length in flies typically matches that of pre-miRNAs, this pathway provides a relatively easy mechanism for the emergence of new miRNAs. Nonetheless, mechanisms likely exist to dampen mirtron activity: mirtrons are expressed at modest levels and are very poorly conserved, consistent with rapid evolutionary birth and death (Berezikov et al., 2010; Chung et al., 2011). But how do flies keep mirtron activity in check? In this issue of *Molecular Cell*, two articles, in investigating miRNA uridylation, unexpectedly shed light on this important, and seemingly unrelated, question (Bortolamiol-Becet et al., 2015; Reimão-Pinto et al., 2015).

To understand 3′ end modifications in flies, Reimão-Pinto et al. (2015) and Bortolamiol-Becet et al. (2015) first turned to high-throughput sequencing of small RNAs. As with other organisms (Scott and Norbury, 2013), uridylation and adenylation of miRNAs in S2 cells and adult flies represented the majority of the modifications. Uridylation was enriched on miRNAs derived from the 3′ side of

Article

Molecular Cell

A Major Role of DNA Polymerase δ in Replication of Both the Leading and Lagging DNA Strands

Graphical Abstract

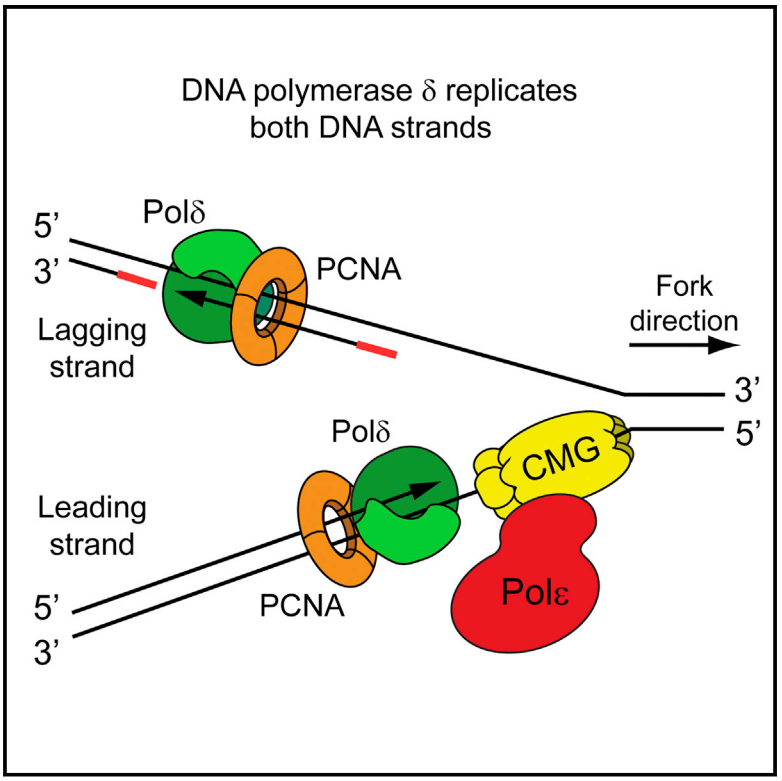

Authors

Robert E. Johnson, Roland Klassen, Louise Prakash, Satya Prakash

Correspondence

s.prakash@utmb.edu

In Brief

The current model of eukaryotic DNA replication suggests that DNA polymerase (Pol)ε primarily replicates the leading strand while Polδ replicates the lagging strand. Johnson et al. provide genetic evidence that Polδ replicates both strands, while Polε's proofreading activity is important for removing Polδ-generated errors from the leading strand.

Highlights

- Polδ-generated errors occur on both the leading and lagging DNA strands
- Polδ errors are removed by mismatch repair, Polε exonuclease, and Exo1
- Polδ replicates both the leading and lagging DNA strands
- Polε does not replicate the leading strand

Johnson et al., 2015, Molecular Cell *59*, 163–175
July 16, 2015 ©2015 Elsevier Inc.
http://dx.doi.org/10.1016/j.molcel.2015.05.038

Molecular Cell
Article

CellPress

A Major Role of DNA Polymerase δ in Replication of Both the Leading and Lagging DNA Strands

Robert E. Johnson,[1,3] Roland Klassen,[1,2,3] Louise Prakash,[1] and Satya Prakash[1,*]
[1]Department of Biochemistry and Molecular Biology, University of Texas Medical Branch, Galveston, TX 77555-1061, USA
[2]Present address: Institut für Biologie, FG Mikrobiologie, Universität Kassel, Kassel D-34132, Germany
[3]Co-first author
*Correspondence: s.prakash@utmb.edu
http://dx.doi.org/10.1016/j.molcel.2015.05.038

SUMMARY

Genetic studies with *S. cerevisiae* Polδ (*pol3-L612M*) and Polε (*pol2-M644G*) mutant alleles, each of which display a higher rate for the generation of a specific mismatch, have led to the conclusion that Polε is the primary leading strand replicase and that Polδ is restricted to replicating the lagging strand template. Contrary to this widely accepted view, here we show that Polδ plays a major role in the replication of both DNA strands, and that the paucity of *pol3-L612M*-generated errors on the leading strand results from their more proficient removal. Thus, the apparent lack of Polδ contribution to leading strand replication is due to differential mismatch removal rather than differential mismatch generation. Altogether, our genetic studies with Pol3 and Pol2 mutator alleles support the conclusion that Polδ, and not Polε, is the major DNA polymerase for carrying out both leading and lagging DNA synthesis.

INTRODUCTION

A number of models have been proposed for the roles of DNA polymerases (Pols) Polδ and Polε in the replication of the two DNA strands. A role for Polδ in the replication of both DNA strands was indicated from studies of SV40 replication (Tsurimoto and Stillman, 1991a, 1991b; Tsurimoto et al., 1990; Waga and Stillman, 1994). The observations that the DNA polymerase activity of Polε is not essential (Feng and D'Urso, 2001; Kesti et al., 1999; Suyari et al., 2012), whereas the polymerase function of Polδ is indispensable for viability (Boulet et al., 1989; Hartwell, 1976; Simon et al., 1991; Sitney et al., 1989), also supported a role for Polδ as the major replicase. However, more recent genetic studies with error-prone variants of yeast Polδ and Polε led to a model whereby Polε primarily replicates the leading DNA strand and Polδ replicates the lagging strand (Larrea et al., 2010; Nick McElhinny et al., 2008; Pursell et al., 2007). This model of asymmetric leading and lagging strand replication by two different DNA polymerases is now widely accepted.

This model relies on data from *Saccharomyces cerevisiae* strains harboring the *pol3-L612M* mutation in the catalytic subunit of Polδ or the *pol2-M644G* mutation in the catalytic subunit of Polε. From the observations indicating the prevalence of signature mutations in the lagging strand in the *pol3-L612M* and the *pol3-L612M msh2Δ* mutant strains, a role for Polδ in the replication of the lagging strand was inferred (Nick McElhinny et al., 2008). And from the prevalence of signature mutations in the leading strand in the *pol2-M644G* mutant, a role for Polε in the replication of the leading strand was deduced (Pursell et al., 2007).

Mismatched base pairs generated during DNA synthesis by the replicative Pols are removed by multiple processes including mismatch repair (MMR), Exo1, and proofreading by the 3′→5′ exonuclease activities of Polδ and Polε. Hence, the relative prevalence of signature mutations on the two DNA strands could be affected either by differential rates of error generation during replication or by the differential action of mismatch removal processes on the two DNA strands. In view of these considerations, we re-examined the roles of Polδ and Polε in the replication of the two DNA strands and show that MMR, as well as Exo1 and Polε exonuclease, compete for the removal of replication errors on both the DNA strands, and that differential error removal rather than differential mismatch generation accounts for the bias of replication errors on the lagging strand in the *pol3-L612M* strain.

Furthermore, the complete absence of Polε signature mutations from the leading strand in the *pol2-M644G msh2Δ* strain supports the conclusion that the DNA polymerase activity of Polε does not significantly contribute to DNA synthesis on the leading strand. In addition to its well-established essential noncatalytic role as a component of the CMG helicase complex, we propose an important role for Polε proofreading exonuclease in the removal of Polδ-generated errors from the leading DNA strand, and suggest that this Polε role can account for all the observations that have been used to implicate a role of Polε in the replication of the leading DNA strand.

RESULTS

Polδ L612M has reduced fidelity and exhibits significant bias for the generation of a T:dGTP mismatch which occurs 28-fold more frequently than the reciprocal A:dCTP mismatch (Nick McElhinny et al., 2007). *pol3-L612M* strains carrying a wild-type *URA3* gene inserted close to *ARS306* in two different orientations in the Δ|(−2)|-7A-YUN1300 genetic background display a highly asymmetric *URA3* to *ura3* hotspot mutational spectrum, wherein the T97C and G764A base substitution

Table 1. Reversion Rates of *ura3-104* in Two Orientations, OR1 and OR2, in the S288C Yeast Strain Carrying *pol3-L612M* in Combination with Mutations in Different Mismatch Removal Processes

Strain	Ura+ rate [$\times 10^{-9}$] (95% CI)	CAG rate [$\times 10^{-9}$] (95% CI)	Numbers of CAG: numbers of GAG+TCG+TTG+AAG
OR2 (T:G on lagging strand)			
WT	2.5 (1.7–3.3)	1.3 (0.9–1.7)	47: 48
pol3L612M	22 (16–28)	21 (15–27)	103: 4
pol3L612M pol2-4	20 (18–22)	19 (17–21)	122: 8
pol3L612M exo1Δ	140 (138–142)	132 (130–134)	116: 7
pol3L612M pol2-4 exo1Δ	440 (395–485)	419 (376–462)	120: 6
pol3L612M msh2Δ	399 (303–495)	396 (301–491)	117: 1
pol3L612M msh2Δ exo1Δ	488 (444–532)	488 (444–532)	124: 0
OR1 (T:G on leading strand)			
WT	2.7 (2–3.4)	1.2 (0.9–1.4)	35: 47
pol3L612M	4.0 (3.8–5.2)	2.4 (1.7–3.1)	57: 36
pol3L612M pol2-4	3.5 (2.8–4.2)	3.5 (2.8–4.2)	121: 0
pol3L612M exo1Δ	22 (21–23)	15 (14–16)	84: 48
pol3L612M pol2-4 exo1Δ	206 (159–253)	206 (159–253)	123: 0
pol3L612M msh2Δ	917 (775–1,059)	896 (758–1,034)	124: 2
pol3L612M msh2Δ exo1Δ	1,172 (942–1,420)	1,143 (901–1,385)	118: 3

See also Figures S5 and S6.

hotspots occurred primarily in one orientation, and the C310T hotspot occurred in the other (Nick McElhinny et al., 2008). Based on the biased fidelity of the mutant polymerase for reciprocal mismatches, these hotspots likely arose via T:dGTP (T-C mutation) and G:dTTP (G-A and C-T mutations) mispairs generated by L612M-Polδ. Since these mutations occurred at high frequency only in the orientation where the hypermutable residue was present in the lagging strand template, Polδ was assigned to primarily replicate the lagging strand (Nick McElhinny et al., 2008). Among the three base change hotspots within *URA3*, the C310T substitution via a G:dTTP mispair occurs at a slightly higher rate than the others (Nick McElhinny et al., 2008) and results in a nonsense TAG codon at position 104, which we refer to as *ura3-104*. Since reversion of *ura3-104 (amber)* back to wild-type Gln-104 would require a T:dGTP insertion in the strand opposite the original G:dTTP mispair which occurred in the forward mutation (see Figure S1A available online), we explored the possibility that the reversion of *ura3-104* would be specifically favored by L612M-Polδ.

ura3-104 Reversion In Vivo in S288C

In vitro synthesis reactions confirmed that, compared to wild-type, the L612M mutant Pol3 catalytic subunit as well as the mutant Polδ holoenzyme inserted dGTP opposite template T preferentially compared to the misinsertion of dCTP opposite template A in the *ura3-104* sequence context (Figures S2A and S2B). The *ura3-104* allele containing the C310T substitution (Figure S1A) was integrated into the yeast genome between the *FUS1* and *HBN1* genes located 1.2 kb left of the highly efficient early firing ARS306 (Nieduszynski et al., 2007) either in the forward (OR1) or reverse (OR2) orientations (Figures S3A and S3B). 2D gel analysis confirms that ARS306 remains a highly efficient origin after integration of *URA3* in the S288C wild-type yeast strain (Figure S4). Thus, in the majority of cells, replication through the *ura3-104* allele will emanate from *ARS306*, thereby replicating T310 on the leading strand in OR1 and on the lagging strand in OR2. In the wild-type background, the *ura3-104* TAG amber codon reverts to Ura3+ at a low rate of $\sim 2.5 \times 10^{-9}$ in both orientations (Table 1). *URA3* spontaneous revertants in OR1 and OR2 displayed nearly equivalent heterogeneity of mutational events at *ura3-104* (Figures S1B and S1C), where in ~43%–50% of Ura+ colonies arose by T310C specific reversion of the TAG codon to CAG (Gln, wild-type sequence), and 49%–56% occurred by conversion to either GAG (Glu), TTG (Leu), or TCG (Ser). Only 1% (2/177) arose by conversion to AAG (Lys), and no TAC (Tyr), TAT (Tyr), or TGG (Trp) (Figure S1C) events were observed. The URA+ revertant colonies harboring Gln, Glu, Leu, or Ser at position 104 exhibit a robust Ura+ phenotype, whereas Ura3 Lys104 colonies were weakly Ura+ (Figure S1B), explaining the low frequency of its recovery. The lack of Tyr or Trp events is likely due to their being Ura− and therefore unrecoverable.

Biased T:dGTP Error Rates in *pol3-L612M* Strains in S288C

Next, we analyzed the reversion frequencies of the *ura3-104* allele in the two orientations (OR1 and OR2) near ARS306 in strains that harbor the *pol3-L612M* mutator allele. Unlike in the *POL3* background where the Ura− to Ura+ reversion rate is similar in both orientations, the reversion rate in the *pol3-L612M* strain is over 5-fold higher when *ura3-104* is in OR2 than in OR1, and where the ura3 T310:dGTP mispair would form during lagging strand synthesis (Table 1). In OR2 *URA3* revertants the ratio of CAG to non-CAG mutational events rose

from ~50% to ~95%, resulting in a 16-fold increase in the specific reversion rate of TAG to CAG in the *pol3-L612M* strain. In contrast, when *ura3-104* was in OR1 in the *pol3-L612M* strain, the CAG-specific reversion rate increased only 2-fold, with a corresponding increase in the occurrence of CAG versus non-CAG events from ~40% to ~60% (Table 1). Thus, although the *pol3-L612M* signature is observed on the leading strand, there is a 9-fold higher rate of the signature on the lagging strand. In contrast to the TAG to CAG mutation, none of the rates of the four other detectable mutation events (GAG, TTG, TCG, and AAG) are significantly increased over wild-type levels in *pol3-L612M* (Figure S3C), which is consistent with the low rate and lack of bias of L612M-Polδ for the generation of the mismatches that lead to these mutations (Nick McElhinny et al., 2007). Based on the CAG specific reversion rates in the *POL3* and *pol3-L612M* strains when *ura3-104* is in OR2, it can be estimated that ~95% of the TAG to CAG mutations in *pol3-L612M* are generated via T:dGTP mismatches by L612M-Polδ during lagging strand replication [(rate CAG *pol3-L612M* OR2 − rate CAG *POL3* OR2)/(rate *pol3-L612M* OR2)]. The strong mutational bias observed for the *pol3-L612M* strains harboring the two orientations of our *ura3-104* reversion system is similar to the results that have been reported for *URA3* to *ura3* forward mutational spectra in a different strain background (Larrea et al., 2010; Nick McElhinny et al., 2008) and is consistent with a role of Polδ in lagging strand, but not in leading strand, replication.

L612M Polδ Generated T:dGTP Errors on the Lagging Strand in S288C

To determine the role of various mispair removal processes in the correction of T:dGMP mispairs generated by L612M-Polδ, we analyzed the frequency and orientation bias of *ura3-104* reversion in *pol3-L612M* strains additionally carrying the *pol2-4* mutation lacking the Polε proofreading exonuclease activity (Morrison et al., 1991); the *msh2Δ* mutation defective in MMR (Johnson et al., 1996); or a deletion of *EXO1*, which contributes to mismatch removal in collaboration with MMR (Genschel et al., 2002; Sokolsky and Alani, 2000; Tishkoff et al., 1997; Tran et al., 1999), individually and in various combinations. All double mutants, including the *pol3-L612M msh2Δ* strain, grow with no apparent defect at 30°C or 37°C and do not display sensitivity to the replication inhibitor HU (Figure S5A). The lack of any significant growth defect in the *pol3-L612M msh2Δ* strain in the S288C genetic background was further confirmed by tetrad analysis of *POL3/pol3-L612M MSH2/msh2Δ* diploids (Figure S5B). Among the triple mutants, the *pol3-L612M pol2-4 exo1Δ* mutant exhibits the same growth phenotype as the double mutants, while the *pol3-L612M msh2Δ exo1Δ* and *pol3-L612M msh2Δ pol2-4* strains display a slow growth phenotype at 30°C and an inability to grow at 37°C (Figure S5A). Growth defects are more severe for the *pol3-L612M msh2Δ pol2-4* strain than for the *pol3-L612M msh2Δ exo1Δ* strain, and both strains exhibit increased sensitivity to HU (Figure S5A). With the exception of *pol3-L612M msh2Δ pol2-4*, we were able to analyze reversion rates and sequence the mutational events at the *ura3-104* amber codon in all of the strains.

In OR2, where the T:dGTP mismatch occurs during lagging strand synthesis, both the *exo1Δ* and *msh2Δ* mutations strongly

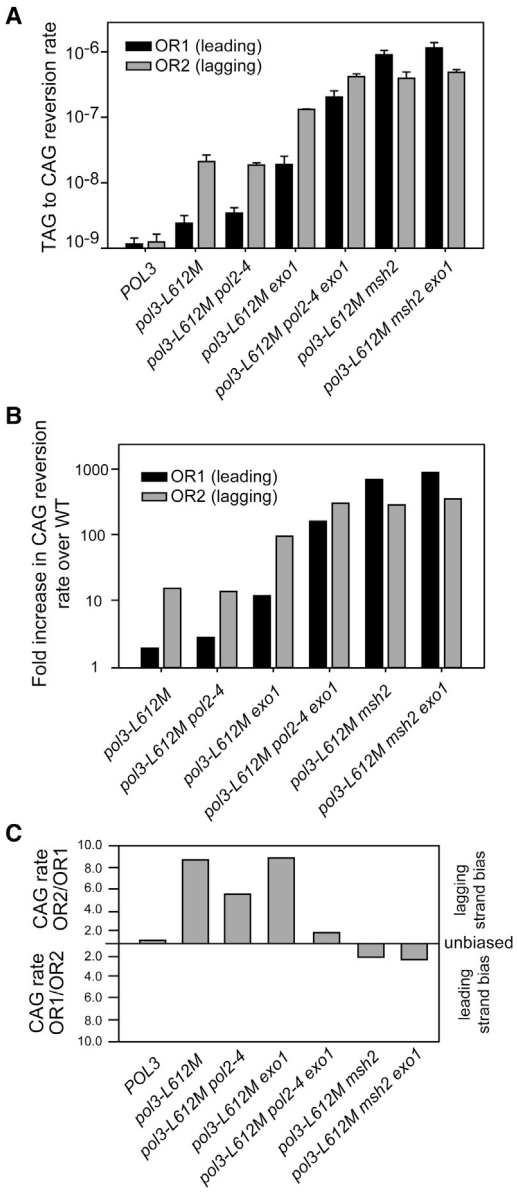

Figure 1. Orientation Bias of *ura3-104* Reversion in the S288C *pol3-L612M* Strains Defective in Polε Proofreading (*pol2-4*), MMR (*msh2Δ*), or Exo1 (*exo1Δ*)

(A) CAG-specific reversion rates of *ura3-104* for various strains in orientations OR1 and OR2. Error bars indicate 95% confidence interval.

(B) Fold increase in CAG-specific reversion rates in either OR1 or OR2.

(C) Reversal of strand bias in Pol3-L612M mutation generation from lagging to leading strand by inactivation of mismatch removal processes.

See also Figures S1–S5.

increase the CAG specific reversion rate, while *pol2-4* on its own has no effect (Table 1; Figures 1A and 1B). In both the *pol3-L612M exo1Δ* and *pol3-L612M msh2Δ* strains, the ratio of CAG versus non-CAG revertants remains strongly biased toward CAG, with non-CAG revertants occurring less than 7% (Table 1). Therefore, Exo1 and MMR efficiently remove T:dGTP mispairs made by L612M-Polδ during lagging strand synthesis, and the

generation of this mispair largely outnumbers the other detectable ones, as expected by the biochemical properties of the mutant polymerase. In the *pol3-L612M msh2Δ exo1Δ* strain, CAG reversion rates in OR2 were not significantly higher than in *pol3-L612M msh2Δ* (Table 1; Figures 1A and 1B), supporting the view that the T:dGTP mispair-correcting activity of Exo1 seen in this assay on the lagging strand occurs in the context of *MSH2*-dependent MMR. The *pol2-4* exonuclease mutation alone did not increase either the total rate or the CAG-specific reversion rate of *ura3-104* by *pol3-L612M*. However, *pol2-4* significantly increased the CAG reversion rate in combination with the *exo1Δ* mutation in the *pol3-L612M* strain (*pol3-L612M pol2-4 exo1Δ* OR2; Table 1; Figures 1A and 1B), suggesting that Polε exonuclease can be recruited to the lagging strand to remove T:dGTP errors generated by Polδ, but that its absence alone can be compensated for by other mismatch removal processes.

L612M-Polδ Generated T:dGTP Errors on the Leading Strand in S288C

Next, we examined the effects of *pol2-4, msh2Δ,* and *exo1Δ*, alone or in different combinations, on the reversion rates in *pol3-L612M ura3-104* OR1, where the T:dGTP mismatch occurs during leading strand synthesis. While the *pol2-4* mutation did not increase the overall *ura3-104* reversion rate, the ratio of CAG to non-CAG events rose dramatically from ~60% to 100% (Table 1), leading to an increase in the CAG-specific reversion rate, suggesting that proofreading by Polε participates in the removal of some *pol3-L612M*-generated T-to-C signature errors on the leading strand. The *exo1Δ* mutation conferred a 6-fold increase in CAG reversion rate over the level seen in *pol3-L612M* alone (Table 1; Figures 1A and 1B). Strikingly, however, the combined absence of Exo1 and Polε exonuclease (*pol3-L612M pol2-4 exo1Δ*) caused an ~85-fold increase in CAG reversion rate, and in a sample size of 123, no non-CAG events were detected (Table 1; Figure 1B). The strong increase of the CAG-specific reversion rate of *ura3-104* in OR1 along with the very low (undetectable) *ura3-104* amber reversion rate via non-T:dGTP errors (GAG, TTG, TCG, and AAG revertants) indicates that L612M-Polδ generates a very considerable amount of replication errors on the leading strand which becomes detectable only after removal of both Polε proofreading and Exo1. Therefore, the proofreading activity of Polε and Exo1 represents redundant functions that remove T:dGTP mismatches generated by L612M Polδ on the leading strand. When CAG-specific reversion rates in OR1 and OR2 are compared, the strong ~9-fold bias toward T:dGTP mismatches occurring on the lagging strand that was observed in *pol3-L612M* alone becomes greatly weakened in *pol3-L612M pol2-4 exo1Δ* (Figure 1C), to only about 2-fold. Since the *exo1Δ* mutation confers a much weaker mutation phenotype than *msh2Δ*, and *MSH2*-dependent MMR remains functional in *exo1Δ* (Tran et al., 1999), the fact that the T:dGTP error rate remains biased on the lagging strand could be due to Exo1-independent MMR being more effective on the leading than on the lagging strand. As discussed below, the results obtained with *msh2Δ* support this possibility.

Inactivation of MMR by *msh2Δ* in *pol3-L612M* conferred an ~370-fold increase in the CAG reversion rate of *ura3-104* (OR1), and the additional removal of Exo1 (*pol3-L612M msh2Δ exo1Δ*) elevated the CAG reversion rate to ~470-fold over the level seen in *pol3-L612M ura3-104* (OR1) (Table 1; Figure 1B). In both cases, the frequency of non-CAG revertants becomes ~2%, indicating again that the large increase in mutation rates is due to the specific T310:dGTP mispair incorporation by L612M-Polδ during replication of the leading strand, which, under normal circumstances, is removed by MMR. Interestingly, the orientation bias in which more T:dGTP errors occur during lagging strand synthesis (OR2) in *pol3-L612M MSH2* is reversed in *pol3-L612M msh2Δ*, where the CAG-specific reversion rate becomes ~2.5-fold higher for T:dGTP mismatch incorporation on the leading strand (OR1) (Table 1; Figure 1C). This result indicates that in the S288C-isogenic strain, MMR is highly effective in the removal of the T:dGTP mismatch at T310 of the *ura3-104* allele on the leading strand. Thus, the higher lagging strand T:dGTP error rate in *pol3-L612M MSH2* was due to biased leading strand MMR rather than biased lagging strand error generation. Since the removal of both Exo1 and Msh2 further elevated CAG reversion rates in *pol3-L612M ura3-104* in OR1, which also increased the OR1/OR2 bias further toward the leading strand error (Table 1; Figure 1C), a function of Exo1-independent MMR on the leading strand cannot be excluded entirely.

Lack of L612M Polδ Mutational Bias in the Replication of Leading and Lagging Strands: Analysis of Forward Mutations in *URA3* in S288C

Our analysis of *ura3*-104 reversion near ARS306 in the *pol3-L612M* strain in the absence of different mismatch removal processes has provided strong evidence that Polδ generates replication errors on both the leading and lagging DNA strands in the S288C strain background. To further confirm this, we carried out forward mutational analyses of *URA3* near ARS306. For each *pol3-L612M* and *pol3-L612M msh2Δ* strain harboring the *ura3-104* allele in OR1 or OR2, the mutant *ura3-104* allele was reverted to the wild-type CAG codon by direct transformation with a DNA fragment containing the *URA3* wild-type sequence. In the *pol3-L612M* OR1 and OR2 strains, the *URA3* to *ura3* forward mutation rates were similar, 1.8×10^{-7} and 1.5×10^{-7}, respectively (Table S1). Sequence analysis of mutations arising in OR1 and OR2, however, was suggestive of lagging strand mutation bias in accordance with L612M Polδ signatures. For instance, C310T mutations, which are predicted to arise from biased G:dTTP mispair generation, were observed in 10 out of 71 mutational events in OR1 (G in lagging), whereas none occurred at this position in 78 mutational events in OR2 (G in leading). Conversely, 9 of 78 mutations in OR2 were T97C mutations (T in lagging), whereas none occurred at this position in OR1 (T in leading). Although in the previous study, the G764A hotspot mutation occurred in an orientation-dependent fashion (Nick McElhinny et al., 2008), in our *pol3-L612M* strains, we observed only 2/71 and 5/78 G764A mutations in OR1 and OR2, respectively, and the overall rate of G to A mutations was only 1.4 times higher in OR2 (G in lagging) than in OR1 (G in leading). All other mutational events observed were either not correlated to the L612M Polδ signature or did not exhibit orientation bias. However, despite lack of bias for G-to-A mutations, the occurrence of the C310T and T97C hotspots is consistent

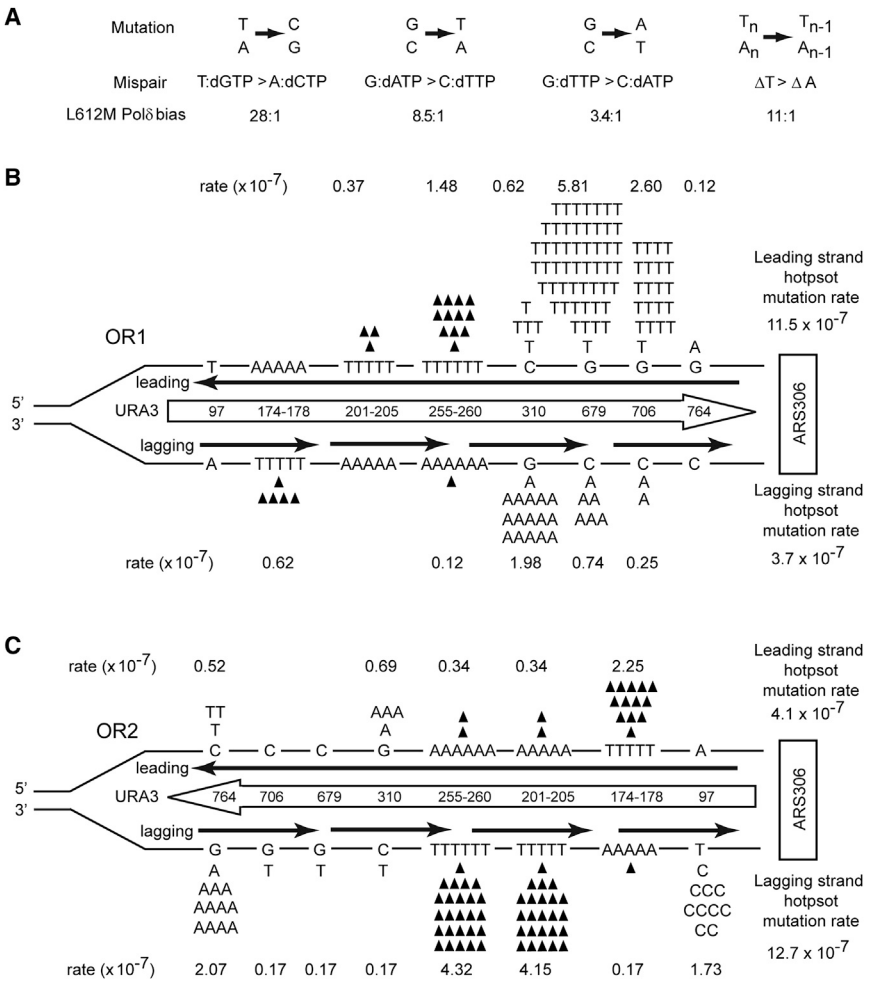

Figure 2. Lack of Strand Bias of *URA3* Mutations near ARS306 in the S288C *pol3-L612M msh2Δ* Strain

(A) Mispair generation bias of L612M Polδ. Point mutations are shown above the two mispairs that generate the mutation. The bias of L612M Polδ for each mispair is given below (Nick McElhinny et al., 2007).

(B) Hotspot mutations in *URA3* observed in OR1 in the S288C *pol3-L612M msh2Δ* strain. The orientation of the *URA3* ORF (boxed arrow) is depicted by the direction of the arrow. *URA3*, integrated ~1.2 kb to the left of ARS306 in chromosome 3, is shown schematically and is not drawn to scale. Each hotspot is shown by their respective base pairs, and their positions in the *URA3* ORF are shown within the boxed arrow. Base changes generated during the replication of the leading strand (above) and the lagging strand (below) are shown. Filled-in triangles represent −1 frameshift mutations. The proportion of observed mutations at each site was assigned to the lagging and leading strand according to the bias for mispair formation by L612M Polδ shown in (A). Strand-specific mutation rates for each site were calculated as described in the text, and the leading and lagging strand hotspot mutation rates given on the far right are the sum of all hotspot mutations on that strand.

(C) Hotspot mutations in *URA3* observed in OR2 in the *pol3-L612M msh2Δ* strain. The orientation of *URA3* is reversed from that in (B).

See also Figures S2, S4, and S5 and Tables S1 and S2.

with the previous study (Nick McElhinny et al., 2008), and together with our mutational analysis of *ura3-104* reversion in the *pol3-L612M* strain, they indicate a prevalence of L612M Polδ signature errors on the lagging strand when MMR is proficient.

Next we analyzed *URA3*-to-*ura3* forward mutations that occur in the *pol3-L612M msh2Δ* strain in OR1 and OR2 orientations in the S288C genetic background. MMR efficiently repairs 1 bp frameshifts, and in the previous study (Nick McElhinny et al., 2008), three orientation specific −1 frameshift hotspots (A174-178, T201-205, T255-260) occurred in *URA3* in the *pol3-L612M msh2Δ* strain and were assigned to L612M Polδ synthesis by correlation to an 11:1 bias for deletions of T over deletions of A (Nick McElhinny et al., 2007). Similar to the *pol3-L612M* single mutant strain, the base changes that dominated the mutation spectra in the *pol3-L612M msh2Δ* strain were the T97C, C310T, and G764A hotspots. Based upon the remarkable asymmetry with which these mutations arose in the two different orientations, and based upon the biased mispair formation spectra of L612M Polδ, the high mutation rates of these hotspots were assigned to have arisen from errors made during lagging strand replication (Nick McElhinny et al., 2008; Nick McElhinny et al., 2007).

For our analyses, we used the same procedure to calculate the leading and lagging strand mutation rates at each hotspot as was used in the previous study (Nick McElhinny et al., 2008). At each hotspot, the proportion of mutations generated in each strand was calculated based on the reciprocal mismatch bias of L612M Polδ (Figure 2A) as determined from mutations generated during DNA synthesis on a *lacZ* substrate (Nick McElhinny et al., 2007). The number of mutations assigned to each strand was divided by the total mutations sequenced and then multiplied by the total mutation rate to give the strand specific mutation rate for each site (Table S2; Figures 2B and 2C). In OR2 where the coding sequence is in the lagging strand, we observe the signature T97C and G764A hotspots (Figure 2C), and these hotspots do not occur in OR1 at any significant rate (Figure 2B); however, we do observe the G-to-A mutations at C310 in OR2 (Figure 2C) that would arise from errors made during leading strand replication. In addition, whereas ΔT(−1) hotspots were observed to occur almost exclusively in the lagging strand in the previous study (Nick McElhinny et al., 2008), we observe frameshift hotspots occurring in both the DNA strands. For instance, in OR2, frameshifts at T(201–205) or T(255–260), which would arise during lagging strand synthesis, occur each at a rate of ~4 × 10^{-7}, whereas frameshifts at A(174–178), where

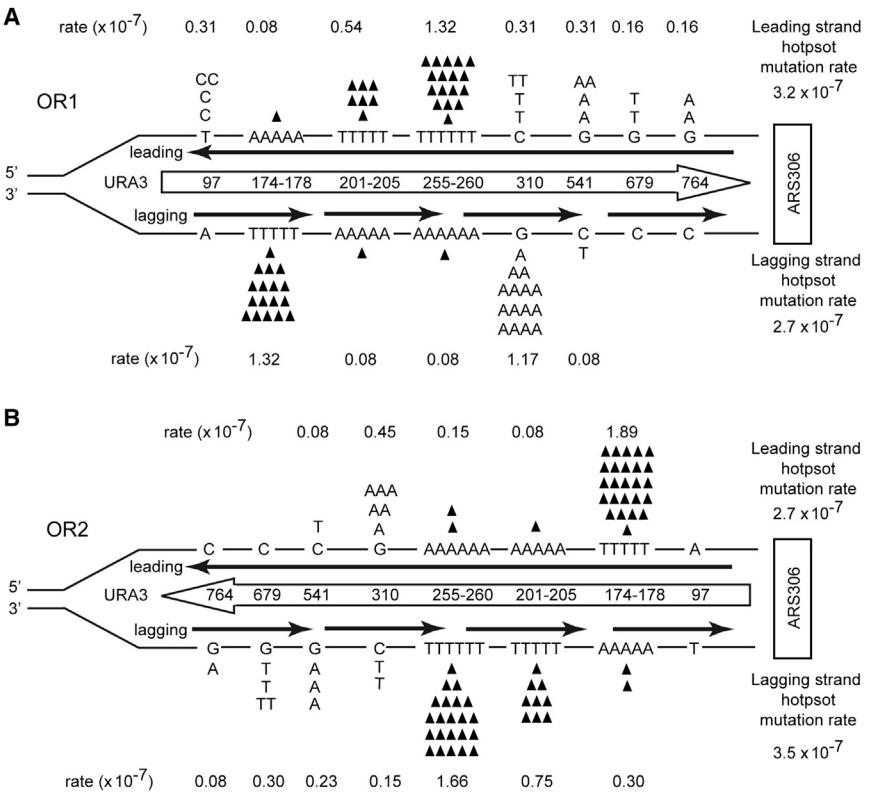

Figure 3. Lack of Strand Bias of *URA3* Mutations Located near ARS306 in the DBY747 *pol3-L612M msh2Δ* Strain

(A) Hotspot mutations in *URA3* observed in OR1 in the DBY747 *pol3-L612M msh2Δ* strain. The *URA3* coding region is integrated ~1.2 kb to the left of ARS306 on chromosome 3 as described in Figure 2.

(B) Hotspot mutations in *URA3* near ARS306 observed in OR2 in the *pol3-L612M msh2Δ* strain. The orientation of *URA3* is reversed from that in (A). The sum of all hotspot mutations for the leading or the lagging DNA strand is given on the right.

See also Figure S4 and Table S3.

the T run is in the leading strand, occur at a rate of ~2 × 10^{-7} (Figure 2C). And in OR1, where T(255–260) occurs in the leading strand, the frameshifts occur at a rate of ~1.5 × 10^{-7} (Figure 2B). Finally, we observe two orientation-specific G-to-T hotspot mutations (G679 and G706) that occur at rates 34 times and 15 times higher in OR1 than in OR2, that were not observed in the previous study (Nick McElhinny et al., 2008). Importantly, L612M Polδ exhibits an 8.5:1 bias for G:dATP mispair formation over the C:dTTP mispair (Nick McElhinny et al., 2007), and we have confirmed that at position 679 in *URA3*, L612M Pol3 exhibits preferential incorporation of an A opposite template G compared to the incorporation of a T opposite template C (Figures S2C and S2D). Therefore, since ~90% of G679T and G706T hotspot mutations can be attributed to having occurred from a G:dATP mispair, the high rate of these two hotspot mutations occurring in OR1 can be assigned to errors made by Polδ during leading strand replication. When OR1 and OR2 strand-specific mutation rates are compared, the total *pol3-L612M* signature hotspot mutation rate of *URA3* in OR1 is ~3-fold higher in the leading strand than in the lagging strand (Figure 2B), while in OR2 the total *Pol3-L612M* signature hotspot mutation rate is ~3-fold higher in the lagging strand than in the leading strand (Figure 2C).

Analysis of Forward Mutations in *URA3* Integrated at Three Different Genomic Locations in the DBY747 Strain

To determine whether our observations were unique to the S288C genetic background or shared by other yeast strains, we examined *URA3* forward mutations in OR1 and OR2 at ARS306 and ARS1 in the DBY747 strain harboring the *pol3-L612M msh2Δ* mutations. In this strain, the genomic copy of *URA3* was deleted to prevent rearrangements with the *URA3* gene integrated near an ARS. In addition to integrating the *URA3* gene in opposite orientations (OR1 and OR2) ~1.2 kb left of ARS306 as was done in the S288C strain, the *URA3* was also integrated in opposite orientations at a second position on chromosome 3, ~10 kb left of ARS306, located in the intergenic region between the *STE50* and *RRP7* genes. In the DBY747 genetic background also we observed no growth defect in the *pol3-L612M msh2Δ* double mutant strain. In this strain we find that, regardless of whether *URA3* was located 1.2 kb or 10 kb left of ARS306 on chromosome 3, individual hotspot mutation sites were far less orientation specific than observed in the S288C background (Tables S3 and S4; Figures 3 and 4). For instance, even though ~74%–80% of all mutations still correlated with the L612M Polδ signatures, the base change hotspot at C310T was observed in both OR1 and OR2 (Figures 3 and 4). By contrast, the hotspot mutation T97C was evident in OR1 at 1.2 kb left of ARS306, whereas none were observed in OR2 at this position (Figure 3). Frameshift mutation hotspots remain highly localized to positions A174–178, T201–205, and T255–260, yet the rates of each are nearly equal in both orientations (Tables S3 and S4; Figures 3 and 4). When the numbers of mutations are allocated to the leading and lagging strands based on the bias of L612M Polδ enzyme and the rates are compared, in either orientation, the rates of *URA3* hotspot mutations on the two DNA strands are nearly identical. For example, at 1.2 kb left of ARS306, the −1 frameshift mutation rate at T255–260 was 1.32 × 10^{-7} on the leading strand in OR1, and 1.66 × 10^{-7} on the lagging strand in OR2 (Figure 3). Similarly, at 10 kb left of ARS306, the T255–260 −1 frameshift rates were 1.09 × 10^{-7} on the leading strand in OR1, and 1.16 × 10^{-7} on the lagging strand in OR2 (Figure 4). The only bias observed was at 1.2 kb left of ARS306 in which there was a ~2.5-fold higher rate of C310T mutations in the lagging strand in OR1 over leading strand mutations in OR2 (Figure 3).

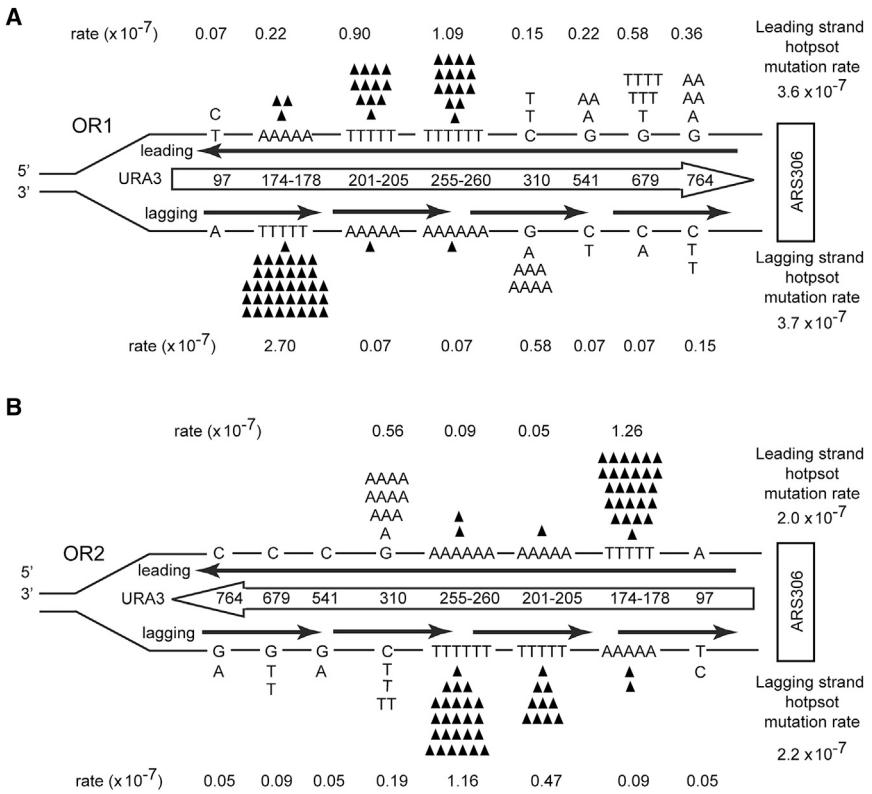

Figure 4. Lack of Strand Bias of *URA3* Mutations Located ~10 kb Left of ARS306 in the DBY747 *pol3-L612M msh2Δ* Strain

(A) Hotspot mutations in *URA3* observed in OR1 in the DBY747 *pol3-L612M msh2Δ* strain. The *URA3* ORF (boxed arrow) is integrated ~10 kb to the left of ARS306 on chromosome 3 in the intergenic region between the *STE50* and *RRP1* genes.

(B) Hotspot mutations observed in *URA3* located ~10 kb to the left of ARS306 in OR2 in the DBY747 *pol3-L612M msh2Δ* strain. The orientation of *URA3* is reversed from that in (A). The sum of all hotspot mutations for the leading or the lagging DNA strand is given on the right.

See also Table S4.

When the total *pol3-L612M*-dependent hotspot mutation rates are compared in either OR1 or OR2 at 1.2 kb or 10 kb left of ARS306, the hotspot mutation rates are nearly identical on the leading and lagging strands (Figures 3 and 4).

To further verify the role of Polδ in the replication of the two DNA strands in the DBY747 *pol3-L612M msh2Δ* strain, we examined forward mutations of *URA3* when integrated near another highly efficient early firing origin, *ARS1*, located on chromosome 4 (Nieduszynski et al., 2007). In this strain also, hotspot mutations occur in both the DNA strands in OR1 and OR2 (Table S5; Figure 5). Overall, in OR1, the leading strand mutation rate of 3.5×10^{-7} was slightly higher than the lagging strand rate of 2.9×10^{-7}, and in OR2, the lagging strand hotspot mutation rate of 7.5×10^{-7} was only 1.7-fold higher than rate of 4.5×10^{-7} in the leading strand (Figure 5).

Thus, at both ARS306 and ARS1 in the S288C and DBY747 strains in the *pol3-L612M msh2Δ* genetic background, although there are some *pol3-L612M*-dependent *URA3* hotspot mutations that occur in an orientation-dependent manner, we do not observe the lagging strand specificity of L612M Polδ signature mutations; rather, we find that L612M Polδ-dependent signature hotspot mutations occur on both DNA strands of *URA3*.

Polε Role in Leading Strand Replication

In view of the strong evidence that L612M Polδ-generated errors occur on both the DNA strands, and that various mismatch removal processes can affect leading strand errors, we re-evaluated the evidence for Polε's role in leading strand replication. The latter was inferred from orientation-biased *URA3* error rates and mutation spectra of a *pol2-M644G* mutator allele of Polε. M644G-Polε generates a T:dTTP mismatch ~40-fold over the reciprocal A:dATP mismatch (Pursell et al., 2007).

First, we examined whether the *pol2-M644G* mutator allele has similar effects on the *URA3* forward mutation spectra in the S288C genetic background. Our *pol2-M644G* strain with intact MMR exhibits a similar *ura3* mutation profile (Figure 6) to the yeast strain used in the previous study (Pursell et al., 2007). For instance, 72% (54 out of 75) of *ura3* mutants were due to A-to-T mutations at the A279 and A686 hotspots when the orientation of *URA3* was such that the noncoding strand T was in the leading strand (OR2) (Figures 6A and 6B). When *URA3* is in the opposite orientation (OR1), however, no hotspot mutations were observed among 43 *ura3* mutants examined, but there is a slight bias for T-to-A mutations, consistent with T:dTMP mispairs being made in the leading strand in this orientation as well. Overall, T:dTMP mispair formation is biased for the leading strand 61:1 in OR2 and 9:1 in OR1 (Figures 6A and 6B). Thus, these data are consistent with the previous report (Pursell et al., 2007) and could indicate that M644G-Polε generates T:dTTP mismatches on the leading strand, but not on the lagging strand. However, since our results with *pol3-L612M* show that MMR and other mismatch removal processes can affect the observed bias for signature mutations on both strands (Table 1; Tables S1 and S2; Figures 1 and 2), we examined how MMR affects the orientation bias of the two hotspots generated by *pol2-M644G* (Figure 6). Surprisingly, in the *pol2-M644G msh2Δ* strain containing *URA3* OR2, where the M644G Polε mutation signature is expected to become higher than in the *pol2-M644G* strain, we observed no hotspot mutations at A279 or A686 in 81 spontaneous *ura3* mutants analyzed (Figures 6A and 6C). Additionally, A-to-T and T-to-A changes occur in only 7% of mutants (6 out of 81) (Figure 6A), and even in these limited cases, the A-to-T bias is toward mutations generated in the lagging strand. Overall, in the *pol2-M644G msh2Δ* strain, we could not detect any *pol2-M644G* signature mutations on the leading strand in the *URA3* gene.

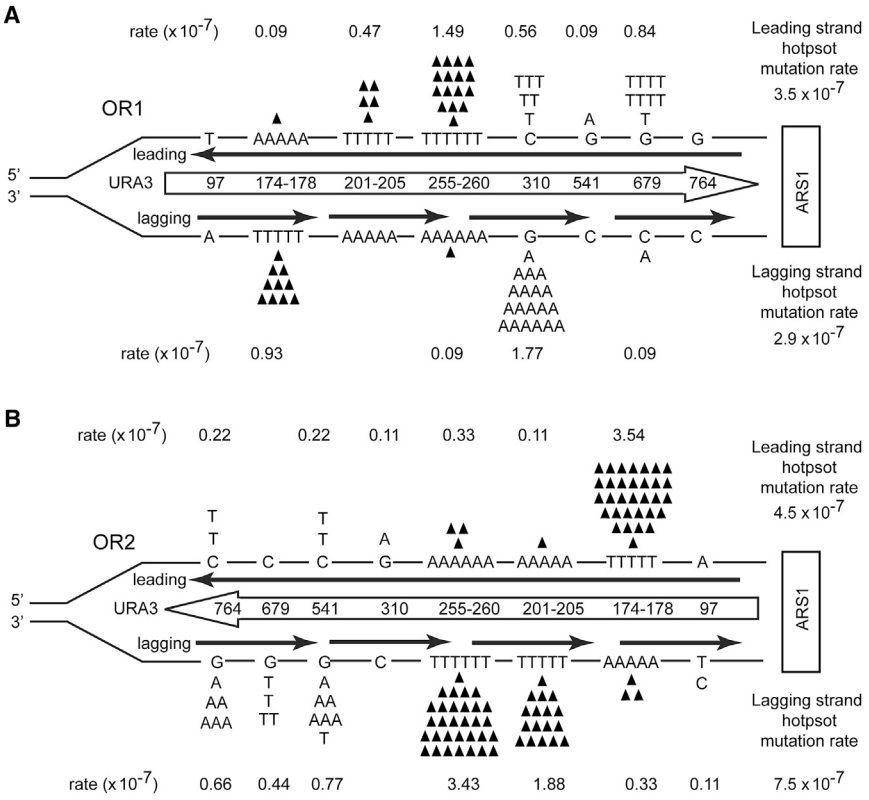

Figure 5. Lack of Strand Bias of *URA3* Mutations in the DBY747 *pol3-L612M msh2Δ* Strain at ARS1

(A) Hotspot mutations in *URA3* observed in OR1 in the DBY747 *pol3-L612M msh2Δ* strain. The *URA3* ORF (boxed arrow) is located ~600 bp to the left of ARS1 on chromosome 4 and is not drawn to scale. Strand-specific mutation rates for each site were calculated as described in the text, and the leading and lagging strand hotspot mutation rates given on the far right are the sum of all hotspot mutations on that strand.

(B) Hotspot mutations in *URA3* near ARS1 observed in OR2 in the DBY747 *pol3-L612M msh2Δ* strain. The orientation of *URA3* is reversed from that in (A).

See also Figure S7 and Tables S5 and S6.

Since there is no orientation-dependent bias in the A-to-T and T-to-A mutations detected in *pol2-M644G msh2Δ* and both of these events are rare compared to other base changes, there is no evidence for Polε having a significant replicative role on either the leading or the lagging strand. Our observation that A-T and T-A errors are infrequent in the *msh2Δ* strain that harbors M644G-Polε, which has been shown to exhibit a high error rate for T:dTTP mismatches in vitro(Pursell et al., 2007), is consistent with the interpretation that Polε has, at best, a minor DNA synthesis role during normal DNA replication.

DISCUSSION

Roles of Polε Exonuclease, Exo1, and MMR in Removing Polδ Errors from Leading and Lagging Strands

The results of our *ura3-104* reversion assay show that signature errors of *pol3-L612M* on the two DNA strands are modulated differentially by mismatch removal processes. For instance, although neither *pol2-4* nor *exo1Δ* strongly increased L612M Polδ's signature error accumulation on the leading strand, the combination of both did so to a large extent (Table 1). On the lagging strand, however, *exo1Δ* alone substantially increased L612M Polδ-dependent error accumulation, and only a modest further increase occurred in combination with *pol2-4*. Therefore, Polε exonuclease and Exo1 act redundantly in error editing on the leading strand, whereas Exo1-dependent mismatch correction is more prevalent on the lagging strand. Additionally, MMR has a very prominent role in correcting L612M Polδ errors from the leading strand (Table 1). Thus, differential error removal rather than differential mismatch generation accounts for the bias of lagging strand errors observed in the *pol3-L612M* strain (Table 1; Figure 1).

Role of MMR in Removing Errors from the Leading and Lagging Strands in Different Yeast Strains

Our analyses of *URA3*-to-*ura3* forward mutations in the S288C and DBY747 *pol3-612M msh2Δ* strains provide additional support for the role of MMR in the correction of L612M Polδ-generated errors on the leading strand. In the S288C background, whereas signature mutations are observed primarily on the lagging strand in the *pol3-L612M* strain (Table S1), signature errors occur on both strands in the *pol3-L612M msh2Δ* strain (Table S2; Figure 2). Although in the *pol3-L612M msh2Δ* strain the L612M Polδ-generated hotspot mutations occur on both DNA strands, the sites at which specific hotspots occur differ in an orientation-dependent manner. This indicates that both MMR and L612M-Polδ mispair generation can act differentially at different sites during replication of the two DNA strands.

In the DBY747 *pol3-L612M msh2Δ* strain, the orientation dependence of site-specific hotspots is greatly diminished, regardless of whether *URA3* was 1.2 or 10 kb away from ARS306. In fact, all the hotspots in *URA3* were observed at various rates in both OR1 and OR2 (Figures 3 and 4). When *URA3* was integrated ~600 bp from ARS1, the only hotspot exhibiting strong orientation dependence was C310T (Figure 5). Thus, in the DBY747 strain, the overall rates of Pol3-L612M-dependent signatures in the MMR-deficient background were nearly equal in the leading and lagging strands. This would suggest that in this strain background, Pol δ-generated mispairs are recognized and removed by MMR from both strands with equal efficiency, unlike that seen in the S288C background.

In summary, our finding that, in both the S288C and DBY747 strains carrying the *pol3-L612M msh2Δ* mutations, L612M Polδ-generated errors occur on both the leading and the lagging DNA strands strongly suggests that Polδ plays a major role in replicating both strands. Furthermore, they indicate that

A

Mutation T→A / A→T

Mispair T:dTTP > A:dATP

M644G Polε bias 39:1

ura3 mutation	$A_{279}T$	$A_{686}T$	Total A to T	Total T to A	Leading:lagging mispair ratio (A to T : T to A)
	T:dTTP location				
OR2	Lead	Lead	Lead	Lag	
pol2-M644G MSH2$^+$	10/75	44/75	61/75	1/75	61 : 1
pol2-M644G msh2Δ	0/81	0/81	2/81	4/81	1 : 2
OR1	Lag	Lag	Lag	Lead	
pol2-M644G MSH2$^+$	0/43	0/43	1/43	9/43	9 : 1
pol2-M644G msh2Δ	0/66	0/66	0/66	4/66	4 : 0

B

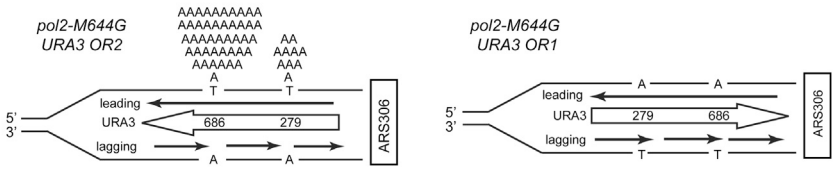

C

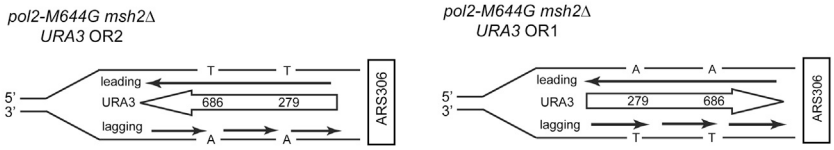

Figure 6. Lack of *pol2-M644G* Signature Errors in MMR-Deficient Strains

(A) Mutational bias for A-to-T and T-to-A mutations in *pol2-M644G* and *pol2-M644G msh2Δ* strains. The T:A-to-A:T mutation is shown above the two mispairs that cause the mutation. The signature bias exhibited by *pol2-M644G* is indicated (Pursell et al., 2007). The number of spontaneous A-to-T and T-to-A mutation events as well as hotspot mutations A279T and A686T in *pol2-M644G* and *pol2-M644G msh2Δ* strains harboring *URA3* in orientation 1 (OR1) or in orientation 2 (OR2) are shown. The location of the T:dTTP mispair in the leading (lead) or lagging (lag) strand in each orientation is shown, and the ratio of leading strand versus lagging strand mutations is given.

(B and C) Schematic representation of the leading and lagging strand-specific mutational events at A279 and A686 in *URA3* in OR1 or in OR2 in the *pol2-M644G* (B) and *pol2-M644G msh2Δ* (C) strain.

mismatch removal processes can act differentially in different yeast strains.

Absence of Polε Signature Mutations in *pol2-M644G msh2Δ*

Our conclusion that Polδ replicates both DNA strands required a re-evaluation of the proposal that Polε replicates the leading strand (Pursell et al., 2007). This inference was based on the mutational bias for T:dTMP mispair formation on the leading strand in the *pol2-M644G* strain (Pursell et al., 2007). A major role of Polε in leading strand replication posits that the prevalence of Polε signature mutations on the leading strand would be greatly elevated in the absence of mismatch removal processes, since Polε-generated errors would not be removed. However, the complete absence of hotspot mutations in the S288C strain carrying the *pol2-M644G msh2Δ* mutations indicates that the signature mutations that were assigned to Polε's role in leading strand replication actually occur at a very low rate. Furthermore, in the *pol2-M644G msh2Δ* strain, even the non-hotspot signature A-T and reciprocal T-A mutations are rare and do not exhibit leading strand preference. In fact, in the OR2 orientation, which exhibited extensive bias in the *pol2-M644G* single mutant, we find a 2:1 bias for T:dTTP mispair formation in the lagging strand in the *pol2-M644G msh2Δ* mutant (Figure 6).

The absence of M644G Polε signature mutations on the leading strand has also been reported for the ΔI(−2)I-7B-YUNI300 strain harboring the *pol2-M644G msh2Δ* mutations (Lujan et al., 2012). Among the ~600 total *ura3* mutants sequenced for the two orientations, there was one A-to-T mutation on each of the DNA strands at A279 and no A-to-T mutation on the leading strand at A686, and a total of only three and two A-to-T mutations were observed on the leading and lagging strands, respectively. Thus, even though M644G Polε exhibits an ~40-fold bias for the formation of T:dTTP mispair over the reciprocal A:dATP mispair, this mutation is almost completely absent in the mutational spectra of the *pol2-M644G msh2Δ* strain. Thus, data in two different yeast strains support the conclusion that the DNA polymerase activity of Polε is not significantly involved in the replication of the leading strand, as previously suggested from the analyses of mutational spectra in *pol2-M644G* alone (Pursell et al., 2007).

Furthermore, the *ura3* A279T and A686T hotspot mutations arise also in yeast harboring the *pol2-4* exonuclease mutant in an orientation-dependent manner identical to that observed in the *pol2-M644G* mutant in the ΔI(−2)I-7B-YUNI300 and S288C strain backgrounds (Williams et al., 2012; our unpublished data). Thus, T:dTTP mispairs in the leading strand occur in the *pol2-4* mutant, in which there is no bias to generate this specific mispair, at rates similar to the *pol2-M644G* mutant strain in which there is a 40-fold bias for T:dTTP mispairs. These observations suggest that T:dTMP hotspot mispairs persist in the *pol2-4* or the *pol2-M644G* mutant strains because they are not removed by either the *pol2-4* or the *pol2-M644G* mutant polymerases (Ganai et al., 2015).

Variability in Strand-Specific Mismatch Correction Processes in Different Yeast Strains

In contrast to our observations indicating a prominent role of MMR in the correction of L612M Polδ errors in *URA3* on both the DNA strands in yeast strains S288C and DBY747, in the prior study in *msh2Δ* cells, L612M Polδ-generated replication errors in the *URA3* gene were restricted to the lagging strand (Nick McElhinny et al., 2008). Subsequently, this observation was extended to the entire genome by deep sequencing analysis

(Larrea et al., 2010). We note that all these other studies used the yeast strain ΔI(−2)I-7B-YUNI300, which was derived from extensive crossings to mutator strains, including to a *pol3*-01 mutator strain that is defective in Polδ 3′→5′ proofreading exonuclease function (Pavlov et al., 2001) and to a *pol2-11* Polε mutant strain and to a DNA repair defective *rad5-G535R* strain (Figure S6); thus, this strain may harbor mutations that may have arisen during its derivation. By contrast, our studies utilized the more commonly used S288C and DBY747 yeast strains. S288C is the principal progenitor of most laboratory yeast strains (Mortimer and Johnston, 1986), and the complete genomic sequence of this strain has been determined.

Two different possibilities could account for the lack of L612M Polδ signature mutations on the leading strand in the absence of MMR in the ΔI(−2)I-7B-YUNI300 strain. The first possibility is that, unique to this yeast strain, Polε and Polδ are restricted to replicating the leading strand and lagging strands, respectively. However, in this strain background, in spite of the very highly elevated bias of M644G Polε for T:dTTP mispair (~40-fold) over the reciprocal A:dATP mispair, there is complete absence of bias for M644G-Polε signature mutations on the leading strand in the *pol2 M644G msh2Δ* strain (Lujan et al., 2012). Since the bias of mutant Polε for T:dTTP mispair exceeds the bias for any of the signature mutations made by mutant Polδ, one would have expected to see a highly elevated level of Polε signature mutations on the leading strand in the *pol2 M644G msh2Δ* strain. The absence of any bias for Polε signature mutations on the leading strand in the ΔI(−2)I-7B-YUNI300 strain, as well as in the S288C strain, therefore is not consistent with the division of labor model of DNA replication. More likely is the second possibility that in the ΔI(−2)I-7B-YUNI300 strain, as seen in the S288C and DBY747 strains, Polδ replicates both DNA strands, and the lack of L612M Polδ signature mutations on the leading strand in the absence of MMR is due to the more efficient removal of Polδ-generated errors by Polε exonuclease on the leading than on the lagging strand. Consequently, L612M-Polδ signature errors would appear to be biased toward the lagging strand, even though the actual mismatch generation frequencies by Polδ were similar on both strands. This explanation would also account for the L612M-Polδ leading strand signature bias observed genome wide, as detected by deep sequencing.

Ribonucleotide Incorporation in the *pol2-M644G Polε* Mutant

In addition to T:dTTP mispair formation bias, the Polε-M644G enzyme exhibits a highly increased capacity for ribonucleotide incorporation in DNA (Lujan et al., 2013; Nick McElhinny et al., 2010). From the observation that, in the absence of RNase H2, ribonucleotides persist in the nascent leading strand in the *pol2-M644G* mutant, it has been inferred that Polε replicates the leading strand (Lujan et al., 2013). However, it is difficult to reconcile this interpretation with our evidence that Polδ participates equally in the replication of both the leading and lagging DNA strands, and with the lack of any evidence for a role of Polε in the replication of the leading strand as deduced from the absence of Polε signature mutations in the *pol2-M644G msh2Δ* strain. This raises the possibility that an explanation other than a role of Polε in the replication of the leading strand accounts for the increased presence of rNMPs in the nascent leading strand in the M644G Polε mutant.

The Polδ 3′→5′ exonuclease lacks the ability to proofread rNMPs (Clausen et al., 2013); however, since Polε exonuclease can excise them (Williams et al., 2012), it would play an important role in their removal from the leading strand. We suggest that in yeast harboring the M644G Polε mutation, because of the reduction in its proofreading activity (Ganai et al., 2015) and because of its highly elevated propensity to extend synthesis from rNMPs incorporated into the nascent leading strand by Polδ (Lujan et al., 2013), the mutant Polε promotes the persistence of rNMPs in the leading strand. Consequently, increased rNMP levels in the nascent leading strand in the *pol2-M644G* mutant in the absence of RNase H2 would not arise from a role of Polε as the major leading strand replicase, but rather from a lack of their removal and from the highly proficient extension of synthesis from rNMPs misincorporated by Polδ.

Roles of Polδ and Polε in DNA Replication in *S. pombe*

From studies with *S. pombe* harboring *Polδ-L591M* and *Polε-M630F* mutations, it was concluded that Polδ replicates the lagging strand and that Polε replicates the leading strand in fission yeast also. For this study, the mutational spectra of a *ura4/ura5* cassette, in two orientations near an active ARS, was analyzed in the *Polδ-L591M* mutant. Mutations were scattered throughout the coding region, and localized hotspots were not observed. However, from the numbers of T:A→C:G and G:C→A:T mutations, predicted to derive from the T:dG and G:dT mispairs, respectively, a role for Polδ in the replication of the lagging strand was inferred (Miyabe et al., 2011). Notably, mutational changes which indicated an elevated bias of Polδ for mispair formation on the leading strand were not considered. In Figure S7, we plot the data provided in their Table 2 (Miyabe et al., 2011), calculated as the percentages of each type of signature mutation apportioned to either leading or lagging strand based upon the bias for mispair formation determined for the *S. cerevisiae* L612M Polδ enzyme (Table S6). Although there is bias for the formation of G:dT (~2-fold) and T:dG (~3- to 8-fold) mispairs on the lagging strand, for the other signature mutations there is either no bias on the lagging strand, or there is evidence for biased mispair formation on the leading strand (Table S6; Figure S7). In particular, for example, are the data for the G:dA mispair, which is formed by mutant Polδ with an 8.5–fold elevated bias over the reciprocal C:dT mispair (see Figure 2A). In the reverse orientation where there is a high prevalence of G to T mutations, there is an ~5-fold bias for the G:dA mispair on the leading strand over the lagging strand (Table S6; Figure S7). Frameshift mutations also suggest the presence of mutant Polδ-dependent mutations on both DNA strands. For example, despite an 11-fold and 17-fold bias of mutant L612M Polδ in the formation of ΔT and ΔG over ΔA and ΔC, respectively (Nick McElhinny et al., 2007), in the reverse orientation, these mutations occur in both strands at similar rates. In the forward orientation, however, there is ~2-fold bias for ΔT in the lagging strand, but a 9-fold bias for ΔG mutations formed in the leading strand (Table S6; Figure S7). Based on the presumption that Polδ synthesizes both strands in *S. pombe*, the total Polδ signature

mutations on both strands should be nearly equal. As calculated from their data, overall, the Polδ signature mutations on the leading strand in the reverse orientation are slightly higher than on the lagging strand, and in the forward orientation they are only ~2-fold higher on the lagging strand than on the leading strand. Thus, altogether, rather than providing definitive evidence for the involvement of Polδ in the replication of only the lagging strand, their data (Miyabe et al., 2011) support a role of Polδ in the replication of both the leading and lagging DNA strands in *S. pombe.*

Furthermore, their analysis of the *ura4-ura5* mutation bias in *polε-M630F* and *polε-M630F msh2Δ* mutants failed to provide any evidence of a bias for Polε signature mutations on the leading strand in *S. pombe* (Miyabe et al., 2011). Nevertheless, a role for Polε in the replication of the leading strand was inferred from the evidence of increased rNMP incorporation in the nascent leading strand in the absence of RNase H2 in the *S. pombe polε-M630F* mutant (Miyabe et al., 2011). However, in view of the evidence indicating the presence of signature mutations on both the DNA strands in the *polδ-L591M* strain (Table S6; Figure S7), and the absence of Polε signature mutations in the *polε-M630F msh2Δ* double mutant, it is difficult to assign a role for Polε in the replication of the leading strand based on the observation of increased rNMP incorporation in the *Polε-M630F* mutant. That is because in *S. pombe* also, increased presence of rNMPs on the nascent leading strand in the *polε-M630F* mutant would result from the propensity of mutant Polε to extend synthesis from rNMPs incorporated by Polδ on the leading strand, and not from its role as a major replicase for the leading strand.

Recently, the genome-wide incorporation of rNMPs in the two DNA strands has been reported for the Polε and Polδ mutants of *S. cerevisiae* and *S. pombe* (Clausen et al., 2015; Daigaku et al., 2015; Koh et al., 2015; Reijns et al., 2015). Similar to previously reported observations (Lujan et al., 2013; Miyabe et al., 2011), these studies indicate a leading strand bias for rNMP incorporation by mutant Polε. As discussed above, these observations can all be explained by the reduced efficiency of mutant Polε for rNMP removal and by its greatly enhanced proficiency for extending synthesis from rNMPs.

Roles of Polε on the Leading Strand

In both the budding yeast and the fission yeast, the N-terminal polymerase domain of the catalytic subunit of Polε is not required for cell viability, whereas the C-terminal domain (CTD) is essential (Feng and D'Urso, 2001; Kesti et al., 1999). The essential role of Polε CTD, but not the polymerase domain, has also been observed for DNA replication in the *Drosophila* imaginal eye disks (Suyari et al., 2012). Elegant genetic studies with a temperature-sensitive mutation in the CTD of the catalytic subunit of Polε (*cdc20-ct1*) in *S. pombe* have shown that Polε plays an essential role in both the assembly and progression of CMG helicase (Handa et al., 2012), which unwinds the DNA duplex by translocating along the leading strand in a 3′→5′ direction (Fu et al., 2011; Ilves et al., 2010; Moyer et al., 2006). Since the CTD of the catalytic subunit of Polε lacks the DNA polymerase function, the DNA polymerization activity of Polε is not required for this essential role.

Recently, the association of replication proteins with the leading and lagging strands of DNA replication forks has been analyzed in yeast using the eSPAN (enrichment and sequencing of protein-associated nascent DNA) method (Yu et al., 2014). Their observations that Polε and Polδ associate preferentially with the leading and lagging DNA strands, respectively, are consistent with the role of Polδ in replicating both strands and with the role of Polε in the progression of CMG complex on the leading strand. The density of Polδ would be much higher on the lagging strand because it is synthesized in a discontinuous manner, and Polε would be restricted primarily to the leading strand because of its CMG associated role. In other recently reported biochemical reconstitution studies, from the observation that Polε binds tightly to the CMG complex and carries out highly efficient synthesis of the leading strand, it has been inferred that the CMG complex recruits Polε for leading strand synthesis (Georgescu et al., 2014; Langston et al., 2014). However, our genetic studies indicating the requirement of Polδ, but not of Polε, for leading strand replication, imply that in vivo, only the noncatalytic role of Polε in the assembly and progression of the CMG complex is utilized for leading strand replication.

The placement of Polε with CMG on the leading strand would enable Polε to function in diverse roles on this DNA strand. Thus, Polε exonuclease could play a more prominent role in the correction of replication errors generated by Polδ on the leading strand than on the lagging strand. Furthermore, since Polδ exonuclease lacks the ability to proofread rNMPs, but Polε exonuclease has this ability, rNMPs incorporated during replication of the leading strand by Polδ would be subject to removal by Polε exonuclease. The placement of Polε on the leading strand would also allow Polε to function as an accessory polymerase, substituting for Polδ in situations where its ability to carry out replication is compromised. For example, Polε could take over synthesis at sites where Polδ replication stalls, and Polε could play an important role in the repair of the leading strand; e.g., at nicks in the template strand, Polε could mediate the repair of strand breaks in coordination with S phase checkpoint (Navas et al., 1995; Sukhanova et al., 2011).

Concluding Remarks

The major findings of this study and their implications are summarized below.

(1) Our observations indicating the prevalence of L612M Polδ-generated signature mutations on both the DNA strands in *pol3-L612M msh2Δ* at different positions in the genome in two different *S. cerevisiae* strains provide positive proof for the conclusion that Polδ replicates both the leading and lagging DNA strands.

(2) In agreement with the role of Polδ in the replication of both DNA strands, genetic analyses with the *pol2-M644G* Polε mutant lacking MMR have failed to provide any evidence for the involvement of Polε in the synthesis of the leading strand.

(3) We provide evidence that in addition to MMR, Polε exonuclease and Exo1 function in the removal of Polδ replication errors from the two DNA strands, and that these different mismatch removal processes can act differentially on the leading and lagging DNA strands. We suggest that yeast strains differ in

the relative contributions of different mismatch removal processes for correcting Polδ errors from the two DNA strands.

(4) Previously, it was concluded that in *S. pombe*, Polδ, and Polε replicate the lagging and leading strands, respectively. A reconsideration of published data, however, implicates a role of Polδ in the replication of both the leading and lagging DNA strands in *S. pombe* also.

EXPERIMENTAL PROCEDURES

Determination of Spontaneous Reversion Rates and Mutational Changes at *ura3-104*

For each strain, 11 independent cultures, each starting from ~50 cells, were grown in 15 ml of YPD medium, washed with water, and plated on SC-ura media. Cell viability was determined from the number of colonies formed on SC media plated from serial dilutions of the original culture. Rates of *ura3-104* reversion were determined from the number of Ura+ colonies by the method of the median (Lea and Coulson, 1949). Five experiments were performed with each strain. For sequence determination, a large number of independent cultures were grown and plated on SC-ura media. One Ura+ colony from each independent culture was subcloned on medium lacking uracil and subsequently patched onto yeast extract-peptone-dextrose (YPD) medium. Genomic DNA was isolated from patches and the *URA3* gene amplified via PCR using oligos LP2221 (5′-GCCCAGTATTCTTAACCCA-3′) and LP2222 (5′-GTGAGTTTAGTATACATGC-3′). Mutations at the *ura3-104* amber codon were then identified by DNA sequencing with oligo LP2221.

URA3 to *ura3* Mutation Rates and Mutational Spectra

Spontaneous forward mutation rates of *URA3* in OR1 and OR2 were determined using the method of the median as described above. For each strain, 15 independent cultures, each starting from ~50 cells were grown in 0.2–3 ml of YPD medium and grown for 3 days. Cells were washed and resuspended in sterile water before plating on synthetic complete (SC) media containing 5-FOA for the S288C strains and on SC-trp media containing 5-FOA for the DBY747 strains. Cell viability was determined as above. For sequence analyses, a large number of independent cultures were grown, washed, and plated on media as described above. A single FOA^r colony from each culture was patched onto YPD. Genomic DNA was extracted, and the *ura3* gene was amplified via PCR as above and PCR products were sequenced using oligos LP2221 and LP2222.

Protein Purification and DNA Synthesis Assays

The *pol3 L612M* mutant protein which was proficient in its proofreading exonuclease or deficient in it was expressed from a *GAL:PGK* promoter, and the wild-type and mutant Pol3 proteins were purified by glutathione Sepharose as described (Swan et al., 2009). The wild-type and L612M mutant Polδ holoenzymes which were proficient in proofreading exonuclease were purified as described (Acharya et al., 2011). DNA synthesis assays were performed at 30°C (Acharya et al., 2011) under conditions indicated in the legend to Figure S2.

SUPPLEMENTAL INFORMATION

Supplemental Information includes Supplemental Experimental Procedures, six tables, and seven figures and can be found with this article at http://dx.doi.org/10.1016/j.molcel.2015.05.038.

ACKNOWLEDGMENTS

This work was supported by National Institutes of Health grant CA107650.

Received: May 28, 2014
Revised: March 20, 2015
Accepted: May 28, 2015
Published: July 2, 2015

REFERENCES

Acharya, N., Klassen, R., Johnson, R.E., Prakash, L., and Prakash, S. (2011). PCNA binding domains in all three subunits of yeast DNA polymerase δ modulate its function in DNA replication. Proc. Natl. Acad. Sci. USA *108*, 17927–17932.

Boulet, A., Simon, M., Faye, G., Bauer, G.A., and Burgers, P.M.J. (1989). Structure and function of the *Saccharomyces cerevisiae CDC2* gene encoding the large subunit of DNA polymerase III. EMBO J. *8*, 1849–1854.

Clausen, A.R., Zhang, S., Burgers, P.M., Lee, M.Y., and Kunkel, T.A. (2013). Ribonucleotide incorporation, proofreading and bypass by human DNA polymerase δ. DNA Repair (Amst.) *12*, 121–127.

Clausen, A.R., Lujan, S.A., Burkholder, A.B., Orebaugh, C.D., Williams, J.S., Clausen, M.F., Malc, E.P., Mieczkowski, P.A., Fargo, D.C., Smith, D.J., and Kunkel, T.A. (2015). Tracking replication enzymology in vivo by genome-wide mapping of ribonucleotide incorporation. Nat. Struct. Mol. Biol. *22*, 185–191.

Daigaku, Y., Keszthelyi, A., Müller, C.A., Miyabe, I., Brooks, T., Retkute, R., Hubank, M., Nieduszynski, C.A., and Carr, A.M. (2015). A global profile of replicative polymerase usage. Nat. Struct. Mol. Biol. *22*, 192–198.

Feng, W., and D'Urso, G. (2001). *Schizosaccharomyces pombe* cells lacking the amino-terminal catalytic domains of DNA polymerase epsilon are viable but require the DNA damage checkpoint control. Mol. Cell. Biol. *21*, 4495–4504.

Fu, Y.V., Yardimci, H., Long, D.T., Ho, T.V., Guainazzi, A., Bermudez, V.P., Hurwitz, J., van Oijen, A., Schärer, O.D., and Walter, J.C. (2011). Selective bypass of a lagging strand roadblock by the eukaryotic replicative DNA helicase. Cell *146*, 931–941.

Ganai, R.A., Bylund, G.O., and Johansson, E. (2015). Switching between polymerase and exonuclease sites in DNA polymerase ε. Nucleic Acids Res. *43*, 932–942.

Genschel, J., Bazemore, L.R., and Modrich, P. (2002). Human exonuclease I is required for 5′ and 3′ mismatch repair. J. Biol. Chem. *277*, 13302–13311.

Georgescu, R.E., Langston, L., Yao, N.Y., Yurieva, O., Zhang, D., Finkelstein, J., Agarwal, T., and O'Donnell, M.E. (2014). Mechanism of asymmetric polymerase assembly at the eukaryotic replication fork. Nat. Struct. Mol. Biol. *21*, 664–670.

Handa, T., Kanke, M., Takahashi, T.S., Nakagawa, T., and Masukata, H. (2012). DNA polymerization-independent functions of DNA polymerase epsilon in assembly and progression of the replisome in fission yeast. Mol. Biol. Cell *23*, 3240–3253.

Hartwell, L.H. (1976). Sequential function of gene products relative to DNA synthesis in the yeast cell cycle. J. Mol. Biol. *104*, 803–817.

Ilves, I., Petojevic, T., Pesavento, J.J., and Botchan, M.R. (2010). Activation of the MCM2-7 helicase by association with Cdc45 and GINS proteins. Mol. Cell *37*, 247–258.

Johnson, R.E., Kovvali, G.K., Prakash, L., and Prakash, S. (1996). Requirement of the yeast *MSH3* and *MSH6* genes for *MSH2*-dependent genomic stability. J. Biol. Chem. *271*, 7285–7288.

Kesti, T., Flick, K., Keränen, S., Syväoja, J.E., and Wittenberg, C. (1999). DNA polymerase ε catalytic domains are dispensable for DNA replication, DNA repair, and cell viability. Mol. Cell *3*, 679–685.

Koh, K.D., Balachander, S., Hesselberth, J.R., and Storici, F. (2015). Ribose-seq: global mapping of ribonucleotides embedded in genomic DNA. Nat. Methods *12*, 251–257, 3, 257.

Langston, L.D., Zhang, D., Yurieva, O., Georgescu, R.E., Finkelstein, J., Yao, N.Y., Indiani, C., and O'Donnell, M.E. (2014). CMG helicase and DNA polymerase ε form a functional 15-subunit holoenzyme for eukaryotic leading-strand DNA replication. Proc. Natl. Acad. Sci. USA *111*, 15390–15395.

Larrea, A.A., Lujan, S.A., Nick McElhinny, S.A., Mieczkowski, P.A., Resnick, M.A., Gordenin, D.A., and Kunkel, T.A. (2010). Genome-wide model for the normal eukaryotic DNA replication fork. Proc. Natl. Acad. Sci. USA *107*, 17674–17679.

Lea, D.E., and Coulson, C.A. (1949). The distribution of the numbers of mutants in bacterial populations. J. Genet. *49*, 264–285.

Lujan, S.A., Williams, J.S., Pursell, Z.F., Abdulovic-Cui, A.A., Clark, A.B., Nick McElhinny, S.A., and Kunkel, T.A. (2012). Mismatch repair balances leading and lagging strand DNA replication fidelity. PLoS Genet. *8*, e1003016.

Lujan, S.A., Williams, J.S., Clausen, A.R., Clark, A.B., and Kunkel, T.A. (2013). Ribonucleotides are signals for mismatch repair of leading-strand replication errors. Mol. Cell *50*, 437–443.

Miyabe, I., Kunkel, T.A., and Carr, A.M. (2011). The major roles of DNA polymerases epsilon and delta at the eukaryotic replication fork are evolutionarily conserved. PLoS Genet. *7*, e1002407.

Morrison, A., Bell, J.B., Kunkel, T.A., and Sugino, A. (1991). Eukaryotic DNA polymerase amino acid sequence required for 3′——5′ exonuclease activity. Proc. Natl. Acad. Sci. USA *88*, 9473–9477.

Mortimer, R.K., and Johnston, J.R. (1986). Genealogy of principal strains of the yeast genetic stock center. Genetics *113*, 35–43.

Moyer, S.E., Lewis, P.W., and Botchan, M.R. (2006). Isolation of the Cdc45/Mcm2-7/GINS (CMG) complex, a candidate for the eukaryotic DNA replication fork helicase. Proc. Natl. Acad. Sci. USA *103*, 10236–10241.

Navas, T.A., Zhou, Z., and Elledge, S.J. (1995). DNA polymerase epsilon links the DNA replication machinery to the S phase checkpoint. Cell *80*, 29–39.

Nick McElhinny, S.A., Stith, C.M., Burgers, P.M., and Kunkel, T.A. (2007). Inefficient proofreading and biased error rates during inaccurate DNA synthesis by a mutant derivative of *Saccharomyces cerevisiae* DNA polymerase delta. J. Biol. Chem. *282*, 2324–2332.

Nick McElhinny, S.A., Gordenin, D.A., Stith, C.M., Burgers, P.M.J., and Kunkel, T.A. (2008). Division of labor at the eukaryotic replication fork. Mol. Cell *30*, 137–144.

Nick McElhinny, S.A., Kumar, D., Clark, A.B., Watt, D.L., Watts, B.E., Lundström, E.B., Johansson, E., Chabes, A., and Kunkel, T.A. (2010). Genome instability due to ribonucleotide incorporation into DNA. Nat. Chem. Biol. *6*, 774–781.

Nieduszynski, C.A., Hiraga, S., Ak, P., Benham, C.J., and Donaldson, A.D. (2007). OriDB: a DNA replication origin database. Nucleic Acids Res. *35*, D40–D46.

Pavlov, Y.I., Shcherbakova, P.V., and Kunkel, T.A. (2001). In vivo consequences of putative active site mutations in yeast DNA polymerases alpha, epsilon, delta, and zeta. Genetics *159*, 47–64.

Pursell, Z.F., Isoz, I., Lundström, E.-B., Johansson, E., and Kunkel, T.A. (2007). Yeast DNA polymerase ε participates in leading-strand DNA replication. Science *317*, 127–130.

Reijns, M.A., Kemp, H., Ding, J., de Procé, S.M., Jackson, A.P., and Taylor, M.S. (2015). Lagging-strand replication shapes the mutational landscape of the genome. Nature *518*, 502–506.

Simon, M., Giot, L., and Faye, G. (1991). The 3′ to 5′ exonuclease activity located in the DNA polymerase δ subunit of *Saccharomyces cerevisiae* is required for accurate replication. EMBO J. *10*, 2165–2170.

Sitney, K.C., Budd, M.E., and Campbell, J.L. (1989). DNA polymerase III, a second essential DNA polymerase, is encoded by the *S. cerevisiae CDC2* gene. Cell *56*, 599–605.

Sokolsky, T., and Alani, E. (2000). EXO1 and MSH6 are high-copy suppressors of conditional mutations in the MSH2 mismatch repair gene of *Saccharomyces cerevisiae*. Genetics *155*, 589–599.

Sukhanova, M.V., D'Herin, C., van der Kemp, P.A., Koval, V.V., Boiteux, S., and Lavrik, O.I. (2011). Ddc1 checkpoint protein and DNA polymerase ε interact with nick-containing DNA repair intermediate in cell free extracts of *Saccharomyces cerevisiae*. DNA Repair (Amst.) *10*, 815–825.

Suyari, O., Kawai, M., Ida, H., Yoshida, H., Sakaguchi, K., and Yamaguchi, M. (2012). Differential requirement for the N-terminal catalytic domain of the DNA polymerase ε p255 subunit in the mitotic cell cycle and the endocycle. Gene *495*, 104–114.

Swan, M.K., Johnson, R.E., Prakash, L., Prakash, S., and Aggarwal, A.K. (2009). Structural basis of high-fidelity DNA synthesis by yeast DNA polymerase δ. Nat. Struct. Mol. Biol. *16*, 979–986.

Tishkoff, D.X., Boerger, A.L., Bertrand, P., Filosi, N., Gaida, G.M., Kane, M.F., and Kolodner, R.D. (1997). Identification and characterization of *Saccharomyces cerevisiae EXO1*, a gene encoding an exonuclease that interacts with MSH2. Proc. Natl. Acad. Sci. USA *94*, 7487–7492.

Tran, H.T., Gordenin, D.A., and Resnick, M.A. (1999). The 3′->5′ exonucleases of DNA polymerases δ and ε and the 5′->3′ exonuclease Exo1 have major roles in postreplication mutation avoidance in *Saccharomyces cerevisiae*. Mol. Cell. Biol. *19*, 2000–2007.

Tsurimoto, T., and Stillman, B. (1991a). Replication factors required for SV40 DNA replication in vitro. II. Switching of DNA polymerase alpha and delta during initiation of leading and lagging strand synthesis. J. Biol. Chem. *266*, 1961–1968.

Tsurimoto, T., and Stillman, B. (1991b). Replication factors required for SV40 DNA replication *in vitro*. I. DNA structure-specific recognition of a primer-template junction by eukaryotic DNA polymerases and their accessory proteins. J. Biol. Chem. *266*, 1950–1960.

Tsurimoto, T., Melendy, T., and Stillman, B. (1990). Sequential initiation of lagging and leading strand synthesis by two different polymerase complexes at the SV40 DNA replication origin. Nature *346*, 534–539.

Waga, S., and Stillman, B. (1994). Anatomy of a DNA replication fork revealed by reconstitution of SV40 DNA replication *in vitro*. Nature *369*, 207–212.

Williams, J.S., Clausen, A.R., Nick McElhinny, S.A., Watts, B.E., Johansson, E., and Kunkel, T.A. (2012). Proofreading of ribonucleotides inserted into DNA by yeast DNA polymerase ε. DNA Repair (Amst.) *11*, 649–656.

Yu, C., Gan, H., Han, J., Zhou, Z.X., Jia, S., Chabes, A., Farrugia, G., Ordog, T., and Zhang, Z. (2014). Strand-specific analysis shows protein binding at replication forks and PCNA unloading from lagging strands when forks stall. Mol. Cell *56*, 551–563.